# Advances in developing noncovalent small molecules targeting Keap1

Marilia Barreca [1,2,†], Yuting Qin [1,†],
Marie Elodie Hélène Cadot [1], Paola Barraja [2],
Anders Bach [1,*]

[1] Department of Drug Design and Pharmacology,
Faculty of Health and Medical Sciences, University of Copenhagen,
Universitetsparken 2, DK-2100 Copenhagen, Denmark
[2] Department of Biological, Chemical and Pharmaceutical Sciences and
Technologies (STEBICEF), University of Palermo, Via Archirafi 32, 90123 Palermo, Italy

Kelch-like ECH-associated protein 1 (Keap1) is a drug target for diseases involving oxidative stress and inflammation. There are three covalent Keap1-binding drugs on the market, but noncovalent compounds that inhibit the interaction between Keap1 and nuclear factor erythroid 2-related factor 2 (Nrf2) represent an attractive alternative. Both compound types prevent degradation of Nrf2, leading to the expression of antioxidant and antiinflammatory proteins. However, their off-target profiles differ as do their exact pharmacodynamic effects. Here, we discuss the opportunities and challenges of targeting Keap1 with covalent versus noncovalent inhibitors. We then provide a comprehensive overview of current noncovalent Keap1-Nrf2 inhibitors, with a focus on their pharmacological effects, to examine the therapeutic potential for this compound class.
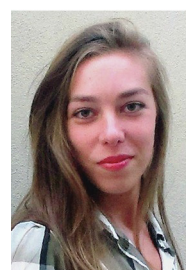
Marilia Barreca received her PhD in medicinal chemistry from University of Palermo (UNIPA) in 2021. During her project she collaborated with the Lymphoma Genomics group at the Institute of Oncology Research (Switzerland), leading to the identification of new [1,2]oxazoles active against different non-Hodgkin lymphoma cells. Since 2021, she is a postdoc at UNIPA, working on design and synthesis of cystic fibrosis transmembrane conductance regulator (CFTR) correctors. In 2022, she joined the Bach group as visiting researcher to work on the development of novel Keap1-Nrf2 protein–protein interaction inhibitors by fragment-based drug discovery.

Yuting Qin received her bachelor degree in Pharmaceutical Analysis from China Pharmaceutical University (CPU) in 2016 and master in Medicinal Chemistry from Ocean University of China (OUC) in 2019. Her previous research focused on metabolism-related diseases, such as pathway study effecting non-alcoholic fatty liver disease (NAFLD), development of liver X receptor-β selective agonists regulating cholesterol homeostasis, and design of hypoxia-inducible factor-2 selective inhibitors modulating tumor metabolism. In 2020, she started her PhD in University of Copenhagen (UCPH) under the supervision of Professor Bach. Her project is about optimization of novel small molecules targeting the Keap1-Nrf2 protein–protein interaction from fragment hits.

Anders Bach received his PhD in medicinal chemistry from UCPH in 2009 in the area of protein–protein interactions and specifically on CNS scaffolding proteins. He continued as postdoc first at UCPH and later at the Italian Institute of Technology working on small-molecule inhibitors of enzymes involved in lipid metabolism and signaling. In 2016, he started his research group at UCPH, where he now holds a position as professor. His group focuses on the use of fragment-based drug discovery to make small-molecule inhibitors of protein–protein interactions involved in oxidative stress and inflammation.

---

* Corresponding author: Bach, A. (anders.bach@sund.ku.dk)
† M.B. and Y.Q. contributed equally to this work.

Introduction

The production and elimination of reactive oxygen species (ROS) are tightly regulated to maintain redox homeostasis, control redox signaling events, and prevent damaging oxidative stress. However, in many diseases, ROS play a central role in inducing inflammation or cellular degeneration, as seen in chronic obstructive pulmonary disease (COPD), atherosclerosis, multiple sclerosis (MS), ischemic stroke, neurodegenerative disorders, sepsis, rheumatoid arthritis, skin diseases, and fibrosis, and by influencing signaling events as seen in hypertension and cancer.[1–3] Classical antioxidant therapy has failed to show consistent and convincing clinical effects, generally due to the inefficiency and lack of capacity of these molecules. A more promising strategy is to upregulate the cells' own antioxidant and cytoprotective enzymes by targeting Kelch-like ECH-associated protein 1 (Keap1).[2,3]

Keap1, an adaptor protein of Cullin 3 (Cul3)-based ubiquitin E3 ligase, and nuclear factor erythroid 2-related factor 2 (Nrf2) are key components of the cellular defense system against oxidative stress and reactive molecules. Keap1 forms a homodimer via its broad complex, tramtrack, and bric-à-brac (BTB) domain, which also attaches to Cul3 and hence mediates the formation of the Cul3-RING E3 ligase (CRL3) complex. Via the two Keap1 Kelch domains in the homodimer, Keap1 binds two peptide motifs from the Neh2 domain of Nrf2, the low-affinity DLG motif, and the high-affinity ETGE motif, thereby facilitating ubiquitination of Nrf2 by CRL3 (Figure 1).[4,5] Thus, by marking Nrf2 for proteasomal degradation, Keap1 keeps Nrf2 levels low under basal conditions. However, Keap1 serves as a sensor for oxidative stress and xenobiotic attacks, as ROS and electrophilic compounds can react with specific redox active cysteine residues on the BTB domain and intervening region (IVR) of Keap1. This leads to a conformational change in the Keap1-Nrf2 complex that perturbs the ubiquitination of Nrf2. Newly expressed Nrf2 then translocates to the nucleus, where it mediates the gene expression of more than 200 detoxifying and antioxidant proteins, thereby exerting its cytoprotective effects (Figure 1).[6–9]

Nrf2 also induces antiinflammatory effects via several mechanisms, including direct suppression of the transcription of the cytokines IL-6 and IL-1β,[10] suppression of stimulator of interferon genes (STING) and hence the type I interferon (IFN) pathway,[11] and by reducing inflammasome activation via regulation of the redox state and lowering the level of key components of inflammasome assembly.[12] Moreover, there is crosstalk between Nrf2 and the pro-inflammatory pathway of the transcription factor nuclear factor-κB (NF-κB).[1,8,13] Nrf2 knockout mice showed increased mortality following endotoxin-induced septic shock and elevated NF-κB transcriptional activity, indicating that Nrf2 exerts antiinflammatory effects by inhibiting NF-κB.[14] Mechanistically, Nrf2 inhibits NF-κB transcription activity by competing with the NF-κB subunit p65 for binding to the shared transcription coactivator CREB-binding protein (CBP)/p300.[15] Additionally, an Nrf2-mediated increase in heme oxygenase-1 (HO-1) leads to higher levels of bilirubin, which inhibits NF-κB
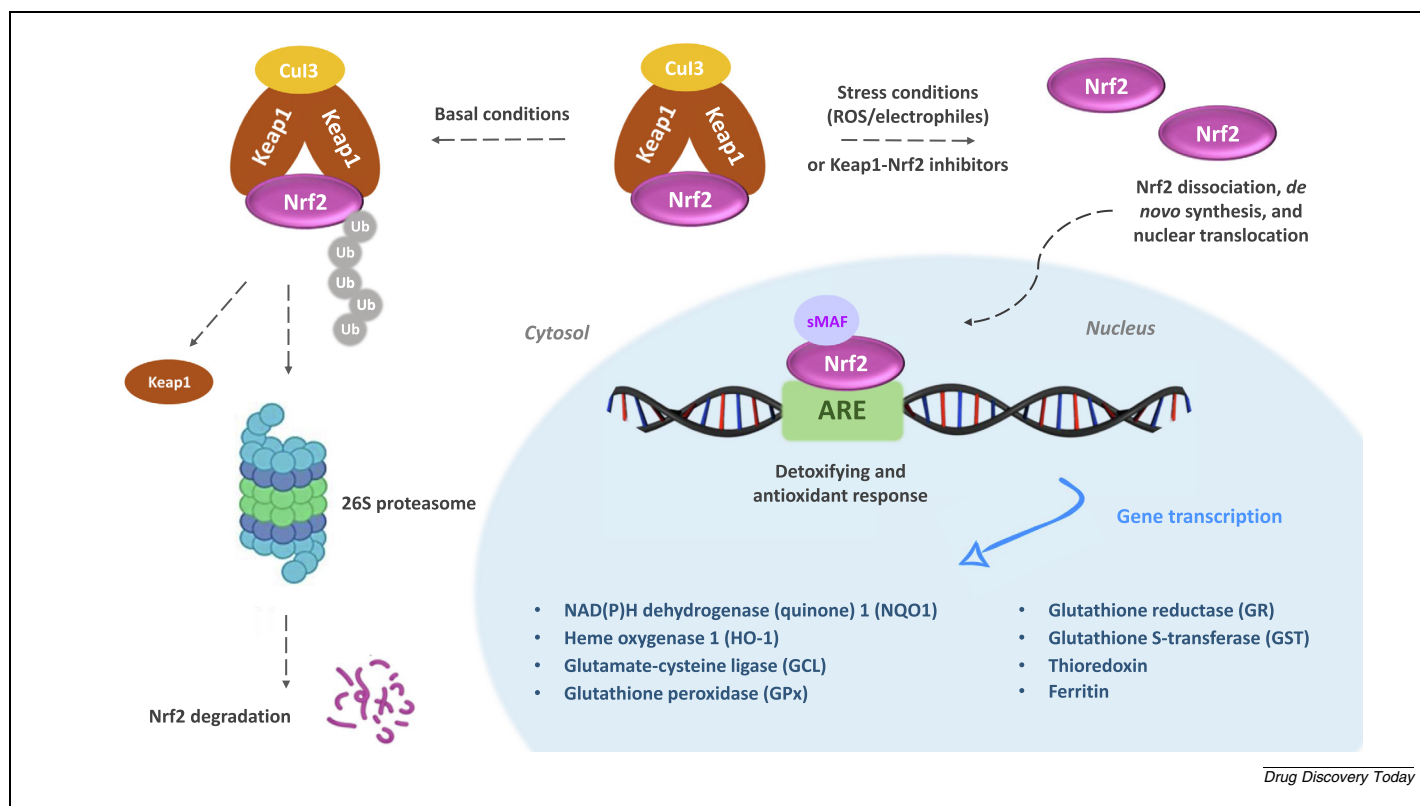
FIGURE 1

Keap1-Cul3-Nrf2 complex: mechanism of action and downstream signals.

transcription of proinflammatory endothelial adhesion molecules.[16] Finally, Keap1 binds inhibitor of NF-κB (IκB) kinase-β (IKKβ) via its Kelch domain and facilitates autophagic degradation and inhibition of IKKβ, which would otherwise phosphorylate and negatively regulate IκB.[13,17]

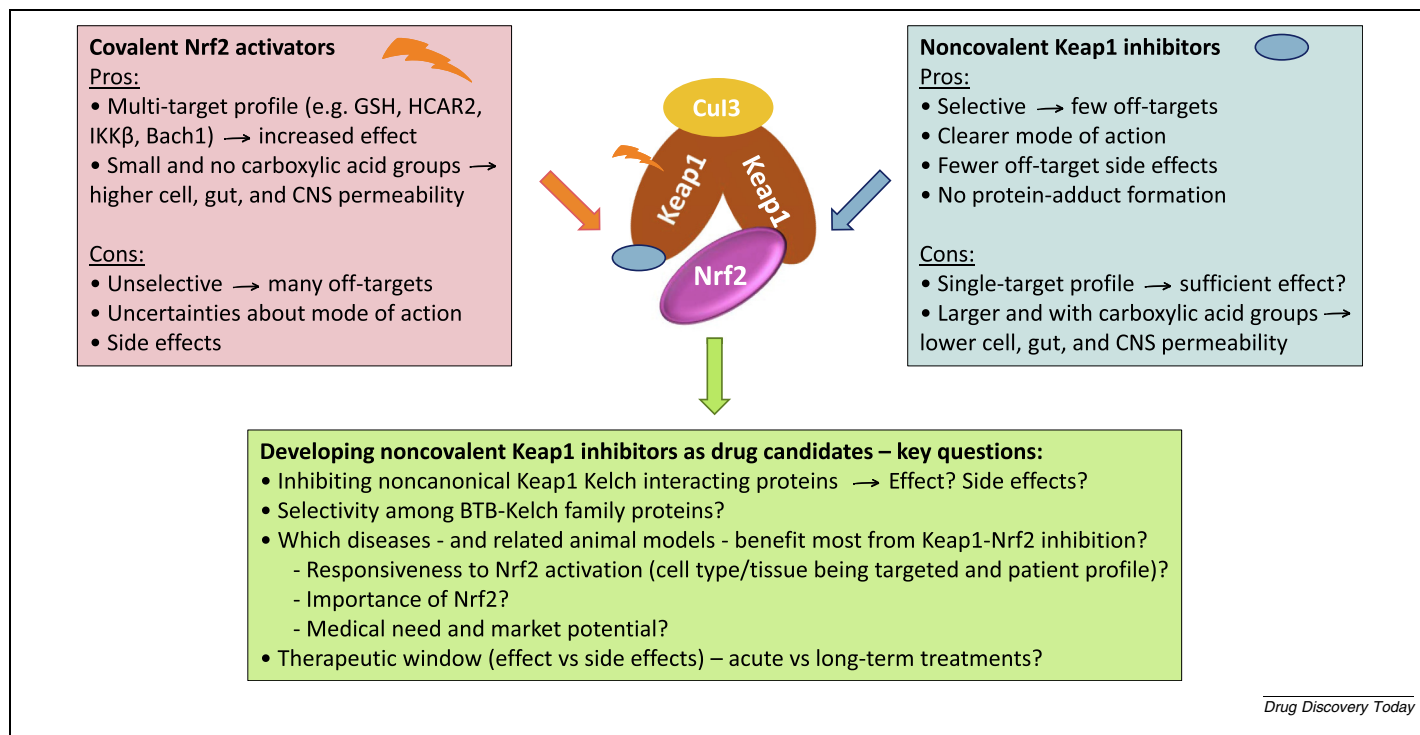## Targeting Keap1: Opportunities and challenges

The central role of Nrf2 in cytoprotective events makes Nrf2 activation an intriguing strategy for drug discovery. There exist a plethora of electrophilic compounds that, similar to ROS and xenobiotics, covalently react with key cysteine residues on Keap1's BTB domain and IVR and thereby activate Nrf2.[3,8] Several such covalent compounds are being tested in clinical trials and three have now been approved as drugs. Dimethyl fumarate (DMF) is used in oral treatments for psoriasis (with other fumarate esters as Fumaderm in Germany and in pure form as Skilarence) and relapsing-remitting MS (Tecfidera).[18] Additionally, the DMF analogue diroximel fumarate is used for MS, and recently, the oleanane triterpenoid omaveloxolone (Skyclarys) was approved for Friedreich's ataxia.[19] Covalent Keap1-targeting compounds may be clinically effective but their unspecific nature leads to uncertainties about their exact mode of action and side effects. DMF reacts with many proteins via the cysteine residues, including 52 T cell proteins and 24 proteins in neurons and astrocytes, many of which are functionally important.[20,21] Several specific Nrf2-independent mechanisms have been elucidated for DMF, including glutathione (GSH) depletion in circulating immune cells leading to the expression of the antiinflammatory HO-1, immunomodulating effects by T cell apoptosis, and activation of the hydroxycarboxylic acid receptor 2 (HCAR2).[22–24] Noticeably, DMF protects against acute inflammation in the experimental autoimmune encephalomyelitis (EAE) MS model of both Nrf2-expressing and Nrf2-deficient mice, suggesting that mechanisms such as GSH depletion and HCAR2 activation are more important than Nrf2 activation.[24–26] DMF side effects include frequent gastrointestinal complaints and flushing, which are responsible for a high withdrawal rate in both psoriasis and MS patients, and potentially a reduction in leukocyte counts, which may be related to the rare cases reported of progressive multifocal leukoencephalopathy (PML).[22,26,27] Omaveloxolone and its analogues, such as bardoxolone methyl (CDDO-Me), which is undergoing clinical trials for chronic kidney disease (CKD) and pulmonary arterial hypertension, are larger and structurally more complex compared with DMF; still, they are unspecific multifunctional compounds. Biotinylated CDDO-Me binds 577 proteins in cells, and several explicit targets and mechanisms besides Nrf2 activation by reacting to Cys151 on Keap1's BTB[28] are known.[29,30] For example, CDDO-Me can bind peroxisome proliferator-activated receptor gamma (PPARγ) and Cys-179 of IKKβ, with the latter leading to inhibition of NF-κB mediated proinflammatory pathways.[31] A phase III trial testing CDDO-Me in CKD patients was terminated due to an increase in heart failure. Later analysis concluded this was a side effect of modulation of the endothelin pathway due to CDDO-Me inhibiting NF-κB, and suggested that this could be circumvented by excluding patients with an ele-

vated baseline level of B-type natriuretic peptide or prior hospitalization for heart failure.[32]

Compounds that noncovalently bind the Keap1 Kelch domain constitute an alternative to the covalent Nrf2 activators, which come with many complexities and challenges as just described. However, so far, no noncovalent Keap1-Nrf2 inhibitors have entered clinical trials. Such compounds displace Nrf2 fully or partly, thereby preventing Nrf2 ubiquitination and proteasomal degradation leading to the expression of Nrf2-controlled genes (Figure 1).[33] Covalent and noncovalent compounds each have their pros and cons, and both come with unanswered questions, as summarized in Figure 2. The Keap1 Kelch pocket is relatively large and contains three arginine residues (Figure 3), whereby high-affinity Kelch binding compounds often become equally large and contain carboxylic acids. These features lower the membrane permeability, oral absorption, and central nervous system (CNS) permeability[4,34,35] and the carboxylic acid can potentially give rise to reactive and toxic phase II metabolites like acyl glucuronides.[36,37] DMF and omaveloxolone do not bear carboxylic acid groups, which is a clear advantage when targeting CNS diseases.

In general, optimized noncovalent compounds have fewer off-targets than covalent ones, and they are less likely to cause toxicity because of protein-adduct formation. On the other hand, noncovalent Keap1 inhibitors may give rise to off-target effects by inhibiting the interactions between Keap1 Kelch and the ~ 15 verified noncanonical Keap1 Kelch-interacting proteins (Figure 2).[38,39] Especially, inhibiting the interaction with IKKβ leads to less degradation of IKKβ, and hence potentially to less control of the proinflammatory NF-κB pathway, and perhaps also to other effects as IKKβ kinase has many substrates.[39] Keap1 also interacts with phosphorylated p62 via its Kelch domain, leading to ubiquitination of p62; this facilitates autophagic degradation of p62's cargo as well as Keap1. However, not much is known about how covalent versus noncovalent Keap1-targeting compounds affect the noncanonical Keap1 substrates or what the functional consequences would be.[3,8,40] Additionally, there exist about 50 BTB-Kelch family proteins besides Keap1 that may be a source of off-targets. However, four well-known and four undisclosed noncovalent inhibitors were recently shown to be highly selective for Keap1 across a panel of 17 human Kelch domain proteins, indicating that selectivity among Keap1 homologues may be less of an issue.[41]

Overall, since the mechanism and off-target profiles of covalent and noncovalent compounds are markedly different (Figure 2), it is difficult to assess the therapeutic potential of noncovalent Keap1-Nrf2 inhibitors based on the clinical progress of covalent Nrf2 activators.[8,40,42] It gives reassurance that pharmacological upregulation of Nrf2 by DMF and omaveloxolone is apparently safe; however, the pharmacodynamic response and adverse reactions are likely different in many ways. Indeed, the promiscuity of the covalent Nrf2 activators could be the reason they are clinically effective, as already discussed for DMF in relation to MS and for CDDO-Me, which inhibits IKKβ. Additionally, CDDO-Me targets and inhibits Bach1, a transcriptional repressor of HO-1, thereby boosting Nrf2-mediated expression of this key antioxidant and antiinflammatory enzyme.[39,43,44]

Covalent Nrf2 activators
Pros:
• Multi-target profile (e.g. GSH, HCAR2, IKKβ, Bach1) → increased effect
• Small and no carboxylic acid groups → higher cell, gut, and CNS permeability

Cons:
• Unselective → many off-targets
• Uncertainties about mode of action
• Side effects

Noncovalent Keap1 inhibitors
Pros:
• Selective → few off-targets
• Clearer mode of action
• Fewer off-target side effects
• No protein-adduct formation

Cons:
• Single-target profile → sufficient effect?
• Larger and with carboxylic acid groups → lower cell, gut, and CNS permeability

Developing noncovalent Keap1 inhibitors as drug candidates – key questions:
• Inhibiting noncanonical Keap1 Kelch interacting proteins → Effect? Side effects?
• Selectivity among BTB-Kelch family proteins?
• Which diseases - and related animal models - benefit most from Keap1-Nrf2 inhibition?
    - Responsiveness to Nrf2 activation (cell type/tissue being targeted and patient profile)?
    - Importance of Nrf2?
    - Medical need and market potential?
• Therapeutic window (effect vs side effects) – acute vs long-term treatments?

Drug Discovery Today

FIGURE 2
Pros and cons of noncovalent Keap1 inhibitors compared with covalent Nrf2 activators. Key questions relevant to the development of noncovalent Keap1 inhibitors as drugs.

Today, whether selective Keap1 Kelch-targeting noncovalent Keap1-Nrf2 inhibitors are effective and safe enough to become future drugs is still an outstanding question. To find out, clinical candidates must be developed and tested in humans, but preclinical evidence supporting further development must be provided first. This comes with key translational challenges, such as identifying the diseases and related animal models that would benefit most from Keap1-Nrf2 inhibition among the many mentioned in relation to oxidative stress, inflammation, and Nrf2 activation.[1,3,8,9] The therapeutic window and responsiveness to Nrf2 activation likely depend on the specific cell type being targeted and the characteristics of the patient population (e.g. age and underlying disease). Additionally, there are concerns about Nrf2 upregulation benefitting existing cancer cells in their defense against ROS and chemotherapeutics. Genetic and pharmacological preclinical results and clinical evidence from DMF trials fortunately refute these concerns. Still, the dose and treatment frequency of the drug, patient profiles, and genetic differences should be considered when assessing the carcinogenic risk.[3,8,40]

Noncovalent Keap1-Nrf2 inhibitors
Developing noncovalent Keap1-Nrf2 inhibitors is a relatively new area of drug discovery.[8] It has been challenged by the large and polar Kelch domain pocket (Figure 3), which makes it difficult to identify high-affinity compounds that also have high cellular potency and druglike properties. Often, shortcomings such as low membrane permeability, solubility, metabolic stability, and bioavailability were seen, not to mention mutagenic activity

and the key challenge of making CNS-active Keap1-Nrf2 inhibitors.[4,45] Some of the earlier compounds were also problematic as they were structurally similar to frequently seen false positives and, accordingly, their activities could not be reproduced.[46] However, as described in recent reviews[42,47,48] and further corroborated herein, consistent medicinal chemistry efforts and ingenious drug design from both academic and industrial laboratories have led to a recent wave of highly promising noncovalent Keap1-Nrf2 inhibitors that combine good target affinity, potency, pharmacokinetic (PK) properties, and activity in various disease models. Here, we provide a comprehensive overview of current noncovalent Keap1-Nrf2 inhibitors and their biological activities, which are also detailed in Table 1. Our aim is to show the status and advances in developing noncovalent Keap1-Nrf2 inhibitors and to examine the therapeutic potential for this intriguing class of compounds.

Tetrahydroisoquinolines (THIQs)
The first noncovalent Keap1-Nrf2 inhibitor was found in 2013 by high-throughput screening (HTS).[49] Originating from a THIQ hit with three chiral centers and modest affinity (IC_{50} = 3 μM) measured in a fluorescence polarization (FP) competition assay, compound **1** (**LH601A**) was found to be the only active diastereomer. Its Keap1-binding activity was confirmed by a competitive surface plasmon resonance (SPR) assay. In cells, compound **1** was active in an antioxidant response element (ARE)-β-lactamase activity reporter assay, induced Nrf2 nuclear translocation,[49] and upregulated Nrf2 target genes and proteins.[50] Later, a structure–activity relationship (SAR) study

Drug Discovery Today
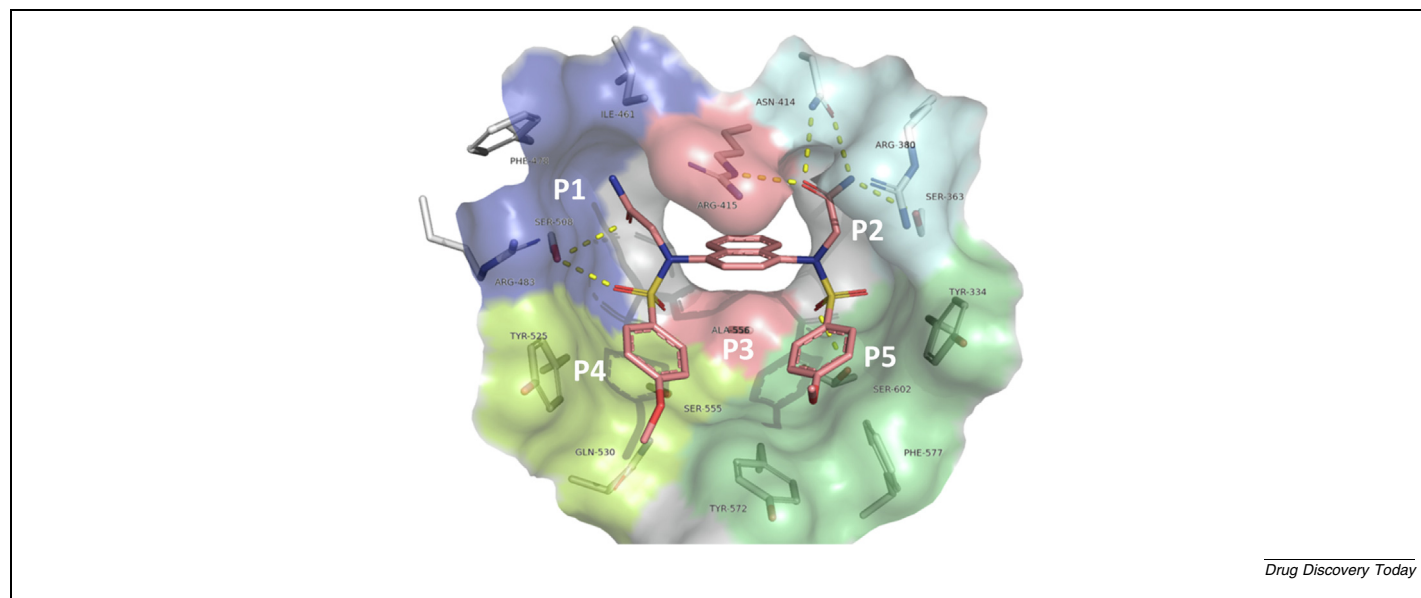
FIGURE 3

Keap1 Kelch subpockets P1–P5 and the interaction with compound **9** (PDB ID 4XMB).[61]

resulted in minor affinity improvements.[51] Interestingly, a series of *in vivo* brain exposure assays of **1** revealed a much higher unbound brain-to-plasma ratio and free brain exposure in Mdr1a/1b/Bcrp knockout mice compared with wildtype mice, demonstrating that **1** is a P-glycoprotein (P-gp) substrate. Replacing the acid with a tetrazole or creating a zwitterionic analogue did not change this but, notably, an acid-containing analogue with lower TPSA showed no efflux and much higher brain exposure; however, it did not bind Keap1. Ontoria *et al.* conducted further optimization of the THIQ series.[52] To generate interactions with the P3 subpocket, analogues bearing glycol or other hydroxyl substituents on the THIQ scaffold were designed by molecular docking. Compound **2** with glycol in position 5 of the THIQ gained fourfold potency compared with **1** in a cell-free time-resolved fluorescence resonance energy transfer (TR-FRET) assay measuring competition between Keap1 Kelch and an Nrf2-peptide. Compound **2** and its carboxamide analogue showed permeability in MDCK-MDR1 cells, with P_{app}(A-B) values of 9 and 46 nm/s, respectively.

Biogen described a series of high-affinity benzotriazole-substituted THIQ compounds.[53] By scaffold hopping and virtual screening, a small library was developed and screened using an Nrf2 nuclear translocation assay in U2O2 cells. After systematic SAR studies and optimization by structure-based drug design (SBDD), compound **3** was obtained with outstanding binding affinity (K_d = 0.7 nM) and good Nrf2 nuclear translocation activity (EC_{50} = 0.36 μM). For comparison, CDDO-Me was about 100-fold more potent than **3** in the translocation assay, but **3** showed a maximum effect threefold higher than CDDO-Me. Compound **3** also potently increased intracellular GSH levels and upregulated Nrf2-regulated genes in human spinal cord astrocytes, and protected the astrocytes from oxidative stress-induced cell death caused by arsenite. Compound **3** had an overall favorable PK profile, including good metabolic stability and oral bioavailability of 20% in rats. However, brain exposure was low, correlating with a relatively high efflux ratio in the MDCK-MDR1 assay. When given orally to mice at doses of 10 and 50 mg/kg, **3** increased mRNA levels of Nrf2 downstream genes in kidney 2–15-fold, dependent on the gene and timing. In the brain, only minor Nrf2-mediated gene activation was observed, which could be explained by the low brain exposure. Interestingly, an analogue of **3** was made by methylating the alpha position of the carboxylic acid. The resulting compound was tenfold more potent by SPR and sixfold better in the Nrf2 translocation assay but unfortunately also showed a tenfold higher efflux ratio in the MDCK-MDR1 assay. In 2020, a series of benzotriazole-substituted THIQs similar to **3** were disclosed in a Chinese patent application.[54] Eight compounds showed IC_{50} values below 50 nM by FP and five had an EC_{50} lower than 1 μM in cells, as exemplified by compound **4**.

Recently, researchers from C4X Discovery Ltd. disclosed about 233 acid-containing THIQ compounds.[55,56] The majority showed excellent inhibitory activity by FP assay (IC_{50} < 10 nM) and potencies in the low or subnanomolar range in a cell assay measuring induction of NAD(P)H dehydrogenase (quinone) 1 (NQO1) gene expression, as exemplified by compound **5**. In a subsequent patent application, the same group focused on replacing the carboxylic acid with substituted amide groups.[57] About 25 out of the 114 compounds had IC_{50} values < 10 nM by FP, including compound **6**. Cell activities generally dropped relative to the acid-containing THIQs, with the six best ones showing EC_{50} values of 18–41 nM. Compounds **5** and **6** were further developed into BRD4-degrading proteolysis-targeting chimeras (PROTACs) (see below).[58]

TABLE 1

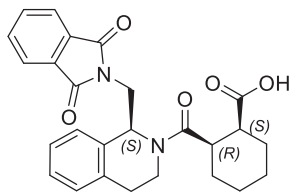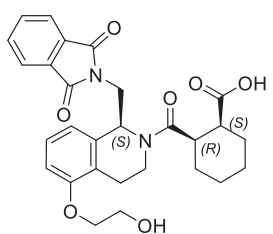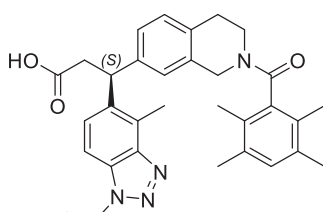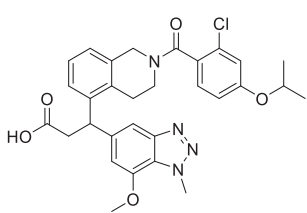**Activities of noncovalent small-molecule Keap1-Nrf2 inhibitors.**
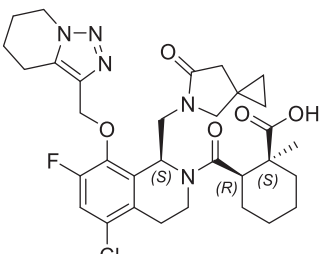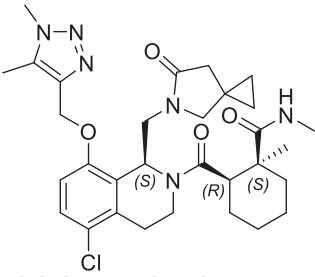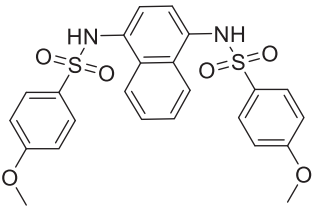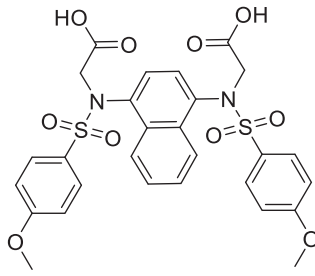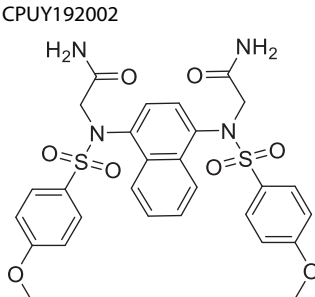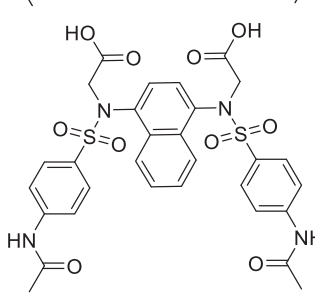
#	Structure	●Affinity ●Cell activity ●DMPK/Tox ●*In vivo* pharmacology	Ref
Tetrahydroisoquinolines (THIQs)			
1	LH601A	● **Affinity:** K_d = 1.0 µM (SPR, competition); IC$_{50}$ = 2.3 µM (FP), 792 nM (TR-FRET) ● **Cell:** EC$_{50}$ = 18 µM in ARE-β-lactamase activity reporter assay (HepG2); EC$_{50}$ = 12 µM in Nrf2 nuclear translocation assay (U2OS); 1.5–5-fold upregulation of Nrf2 target genes (HO-1, TRX1, and NQO1) and fourfold increased protein levels (HO-1, TRX1) @50–100 µM (HEK293). ● **DMPK/Tox:** efflux ratio in MDCK-MDR1 cells: 20; *in vivo* mouse brain exposure: unbound brain-to-plasma (B$_u$/P$_u$) ratio < 0.01 (wildtype) and 0.4 (Mdr1a/1b/Bcrp knockout); free brain exposure (C$_{max}$) < 0.01 µM (wildtype) and 0.18 µM (Mdr1a/1b/Bcrp knockout); cell viability: 100%@100 µM (24 h; HEK293)	49–52
2		● **Affinity:** IC$_{50}$ = 183 nM (TR-FRET) ● **DMPK/Tox:** P$_{app}$(A-B) = 9 nm/s (MDCK-MDR1)	52
3		● **Affinity:** K_d = 0.7 nM (SPR) ● **Cell:** EC$_{50}$ = 0.36 µM (Nrf2 nuclear translocation assay; U2OS cells); EC$_{50}$ = 9.2 nM (GSH levels; astrocytes); 3–6-fold upregulation of Nrf2 target genes (GCLC, OSG1N1, and NQO1) @10–1000 nM (astrocytes); EC$_{50}$ = 51 nM (protection from arsenite; astrocytes). ● **DMPK/Tox:** no CYP (3A4, 2D6, 2C9, 2C8, 2C19, 2B6 and 1A2) inhibition @10 µM; no hERG inhibition @30 µM; stability in hepatocytes: %Q$_h$ = 17.9/<10 in rat/human; MDCK-MDR1 P$_{app}$(A-B) = 7.1 nm/s and efflux ratio = 29.9; *in vivo* PK (rats): 1 mg/kg IV dosing led to AUC of 2510 ng*h/mL and CL of 6.16 mL/min/kg; 5 mg/kg PO led to AUC of 2720 ng*h/mL, t$_{1/2}$ = 3.77 h, and F = 20%; K$_{p,\,uu}$ in mouse 0.04 ● ***In vivo* pharmacology:** 2–15-fold upregulation HMOX1, NQO1, CBR3, OSGIN1 in kidney @10/50 mg/kg (PO; C57BL/6 female mice)	53
4		● **Affinity:** IC$_{50}$ = 17 nM (FP) ● **Cell:** EC$_{50}$ < 1 µM (ARE luciferase assay; HEK293)	54
5		● **Affinity**: IC$_{50}$ = 3.6 nM (FP) ● **Cell**: EC50 = 0.022 nM (upregulation of NQO1 mRNA; BEAS-2B)	55

TABLE 1 (*CONTINUED*)

#	Structure	•Affinity •Cell activity •DMPK/Tox •*In vivo* pharmacology	Ref
6		• **Affinity:** IC$_{50}$ = 6.1 nM (FP) • **Cell:** EC$_{50}$ = 18 nM (upregulation of NQO1 mRNA; BEAS-2B)	[57]

1,4-Diaminonaphthalenes and analogues

#	Structure	•Affinity •Cell activity •DMPK/Tox •*In vivo* pharmacology	Ref
7		• **Affinity:** IC$_{50}$ = 2.7 μM (2D-FIDA) and 1.46 μM (FP); K_d = 1.69 μM (BLI) • **Cell:** sevenfold induction @100 μM (ARE-luciferase reporter assay; DLD1); upregulation of Nrf2 and NQO1 @20 μM (DLD1)	[59–61]
8	 CPUY192002	• **Affinity:** IC$_{50}$ = 28.6 nM (FP), K_d = 3.59 nM (BLI), K_d = 20 nM (SPR) • **Cell:** 3–15-fold induction @0.1–10 μM (ARE-luciferase reporter assay; HepG2); 3–37-fold upregulation of HO-1, GCLM, and NQO1 genes @0.1–10 μM (HCT116) • **DMPK/Tox:** no cytotoxicity; solubility: 0.388 mg/mL (or 440 μM); ∼100% left@20 min (mouse and human liver microsomes)	[60–62,77]
9		• **Affinity**: IC$_{50}$ = 63 nM (FP), K_d = 44 nM (SPR) • **DMPK/Tox:** solubility = 22 μM (low); 0% left@20 min (mouse and human liver microsomes)	[61,77]
10	 CPUY192018	• **Affinity:** IC$_{50}$ = 14.4 nM (FP); K_d value = 39.8 nM (ITC) • **Cell:** – 3–11-fold induction @0.1–5 μM (ARE-luciferase reporter assay; HepG2); upregulation of Nrf2-regulated cytoprotective proteins @10–20 μM (NQO1, HO-1, GCS; HCT116); increased Nrf2 translocation @10 μM (NCM460 colonic cells); upregulation of Nrf2, HO-1, GCLM, and GPx2 genes (2–10-fold) and proteins @1–10 μM (NCM460); protection against DSS-induced oxidative injury @1–20 μM (NCM460) – 5–7-fold upregulation of HO-1, NQO1, and GCLM mRNA @10 μM (HK-2); increase of SOD, CAT, and GPx2 levels and activity @1 μM (HK-2); suppression of ROS @10 μM (HK-2); protect against LPS-induced cytotoxicity @10 μM (HK-2); inhibition of NF-κB activation and suppression of inflammatory factors (TNF-α, IL-18, IL-1β, IL-6, and NO) @1–10 μM (HK-2) – Nrf2 increase and nuclear translocation @50 μM (human retinal endothelial cells, HREC, and RAW264.7 macrophages); increase of NQO1, HO-1, GCLM, GSTM1 and decrease of ROS @50 μM (HREC); reduction of LPS-induced expression of TNF-α @50–500 μM (THP-1) and of AMWAP @0.5–5 μM (RAW264.7 macrophages)	[62–66]

TABLE 1 (*CONTINUED*)
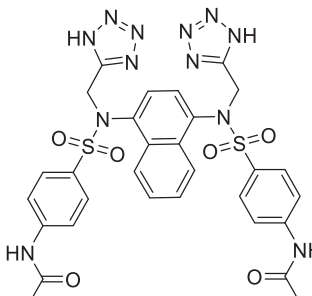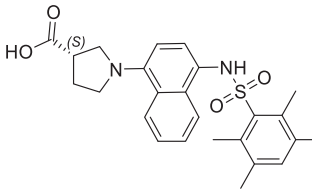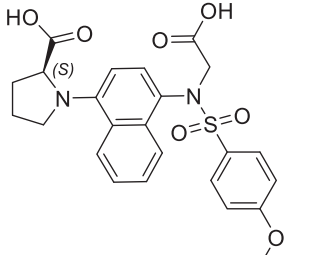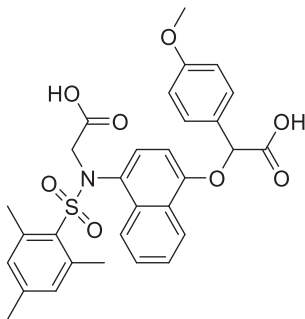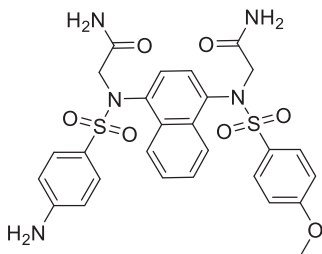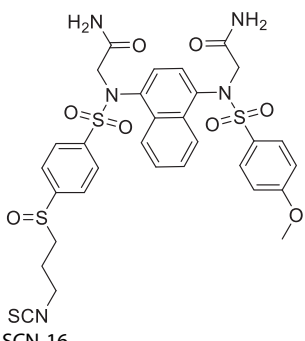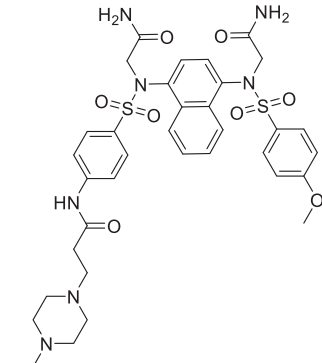
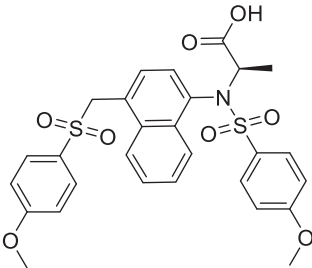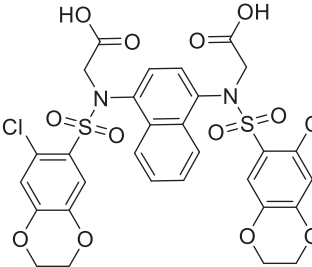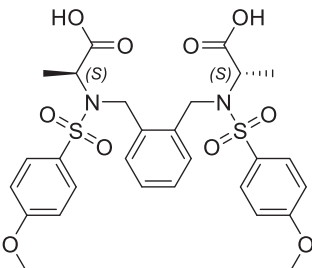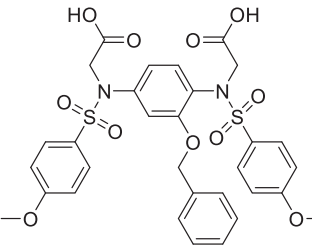| #	Structure	•Affinity •Cell activity •DMPK/Tox •*In vivo* pharmacology	Ref
		– Upregulation of Nrf2 and Nrf2-dependent genes (HO-1, NQO1, GST), increased Nrf2 nuclear translocation @0.1–20 µM, glycolysis suppression, and enhanced phagocytosis of bacteria @10 µM (mice COPD alveolar macrophages) • **DMPK/Tox:** solubility: 5.0 mg/mL; no toxicity or bodyweight change in mice during pharmacology studies; $t_{1/2}$ = 11 min (IV, 1 mg/kg), 22 min (SC, 10 mg/kg) (rats) • *In vivo* **pharmacology**: – Reduction of proinflammatory cytokines (TNF-α, IFN-γ, IL-6, IL-12, and IL-17) in LPS-challenged mice (10 or 80 mg/kg/day, 3 days of pretreatment before LPS; female C57BL/6); attenuated symptoms, reduced inflammatory cytokines (TNF-α, IFN-γ, IL-6, IL-1β) and MPO activity in colon, increased expression of Nrf2-targeted proteins (HO-1, GCLM, and GPx2), and decreased ROS in the DSS-induced mouse model of UC (10/40 mg/kg/day, oral gavage, 64 days) – Alleviation of oxidative stress injury and pathological alterations in LPS-induced chronic renal inflammation mice (IP, 5/20 mg/kg/day, 8 weeks; female C57BL/6) – Increased expression of GSTM1, TXNRD1, and NQO1 (10 mg/kg) and retinal neuroprotection (SC, 10 mg/kg systemic and topical, 1 mg/kg) in rats with retinal I/R injury – Increased OCR/ECAR ratio and phagocytosis of alveolar macrophages and reduced plasma cytokines (TNF-α, IFN-γ, IL-5, IL-6) @0.1 µM (CSC-induced COPD mice)	
11		• **Affinity:** IC_{50} = 15.8 nM (FP) • **Cell:** 2–15-fold induction @0.01–5 µM (ARE-luciferase reporter assay; HepG2); 5–30-fold upregulation of HO-1, GCLM, and NQO1 mRNA @0.1–10 µM and upregulation of NQO1, HO-1, and γ-GCS protein @1–10 µM (HCT116) • **DMPK/Tox:** compound **11** *vs* **10**: pK_a = 5.12 *vs* 4.79; $logD_{7.4}$ 2.31 *vs* 1.02; solubility = 3.5 mg/mL *vs* 5.0 mg/mL; P_e = 42 *vs* 0.3 $\times$ 10^{-6} cm/s (PAMPA)	67
12	 RA839	• **Affinity:** IC_{50} = 140 nM (FP); K_d = 6 µM (ITC) or 0.47 µM (SPR) • **Cell:** fivefold induction @49 µM (ARE-luciferase reporter assay; HepG2); EC_{50} = 1.2 µM in Nrf2 nuclear translocation assay (U2OS); regulated 105 mRNA sets @10 µM (BMDM); reduced NO release and NOS2 mRNA and 40-fold-increased NQO1 mRNA @5–20 µM (LPS-treated BMDM) • **DMPK/Tox:** turnover rate of 99%, 90%, and 76% in microsomes after 20 min in human, mouse, and rat, respectively; no activity against 93 potential off-targets (CEREP safety panel) @10 µM; no effect on cell viability (lactate dehydrogenase release; BMDM) • *In vivo* **pharmacology:** 2–3-fold upregulation of hepatic GCLC and NQO1 mRNA in mice treated with an inhibitor of oxidative hepatic metabolism (IP, 30 mg/kg; male C57/Bl6 mice)	46,68
13		• **Affinity:** IC_{50} = 43 nM (FP); K_d = 53.7 nM (ITC) and 28.5 nM (BLI) • **Cell:** 4–11-fold induction @5–20 µM (ARE-luciferase reporter assay; HepG2); target engagement in cells @10 µM (CETSA) and upregulation of Nrf2, HO-1, NQO-1, and GCLM mRNA (2–12-fold; 8–48 hours) and protein @1–10 µM (hepatic L02); reductions in apoptosis rate (from 49% to 18%), cytokines (IL-1β, IL-6, and TNF-α), and hepatic injury markers (MDA, ALP, and ALT), and upregulation of GSH/GSSG @5–10 µM (12 h pretreatment; APAP-induced toxicity in L02)	69

TABLE 1 (CONTINUED)
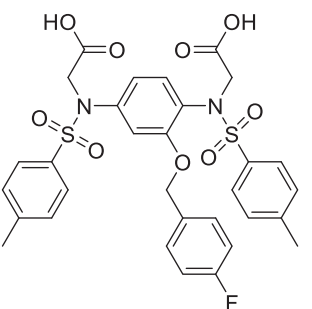
#	Structure	●Affinity ●Cell activity ●DMPK/Tox ●In vivo pharmacology	Ref
14		● **DMPK/Tox:** no cytotoxicity (1–100 μM; L02) ● **In vivo pharmacology:** prevention of APAP-induced hepatotoxicity (expression of Nrf2, HO-1, NQO1, and GCLM; decrease of ROS, MDA, MPO, ALT, ALP, TBIL, IL-1β, IL-6, and TNF-α levels; decreased liver pathology) (IP, 10/40 mg/kg, 24 h before APAP; C57BL/6 female mice) ● **Affinity:** IC_{50} = 75 nM (FP); K_d = 24 nM (ITC) and 36.5 nM (BLI) ● **Cell:** 3–13-fold induction @1–20 μM (ARE-luciferase reporter assay; HepG2); Nrf2 nuclear translocation @10 μM (RAW264.7); 4–6-fold upregulation of HO-1, NQO-1, and GCLM mRNA and increased expression of Nrf2, HO-1, NQO-1, and GCLM @5–10 μM (RAW264.7); reduced ROS levels, restoration of GSH/GSSG, reduction of MPO and cytokines (IL-1β, IL-6, and TNF-α) @1–10 μM (LPS-treated RAW264.7) ● **DMPK/Tox:** $t_{1/2}$ > 10 h (rat liver microsomes); IC_{50} > 10 μM (CYP inhibition); $t_{1/2}$ = 1.72 h (IV, 1 mg/kg; rats) ● **In vivo pharmacology:** diminished serum levels of IFN-γ, IL-1β, IL-6, and TNF-α (IP, 10/40 mg/kg; LPS-treated mice)	70
15	 NXPZ-2	● **Affinity:** K_i = 95 nM (FP); EC_{50} = 120–170 nM (AlphaScreen) ● **DMPK/Tox:** no effect on cell viability @2–200 μM over 24 h (CCK-8; primary cortical neurons); no obvious toxic effects on heart, liver or kidney after in vivo studies (histology); solubility = 55.4/58.6 μg/mL (free/salt, pH 7) ● **In vivo pharmacology:** improved cognitive function and restoration of hippocampal cell number and morphology @53–210 mg/kg (daily PO doses for 7 days; behavioral models of Aβ$_{1-42}$-induced AD mice) (no effect of NXPZ-2 in Nrf2$^{-/-}$ mice); also observed in same mice: Nrf2 levels increased in serum, hippocampus, and frontal cortex; Nrf2 nuclear translocation, increased Nrf2-ARE binding, and decreased oxidative stress (higher levels of GSH, SOD, HO-1, NQO-1; lower levels of malondialdehyde) in hippocampus and cortex; decreased levels of AD markers (p-Tau in hippocampus and cortex, serum Aβ$_{1-42}$)	71,73
16	 SCN-16	● **Affinity:** K_d = 0.455 μM (FP) ● **Cell:** Nrf2 nuclear translocation, HO-1 and NQO-1 induction, and reduction of ROS, NO, and TNF-α @10 μM (LPS-induced mouse peritoneal macrophages; effects greater than **15**/NXPZ-2) ● **DMPK/Tox:** no cytotoxicity @10 μM over 24 h (CCK-8; mouse peritoneal macrophages) ● **In vivo pharmacology:** Nrf2 nuclear translocation, reduced cytokine levels (TNF-α, IL-1β, IL-6) in bronchoalveolar lavage fluid, and reduced lung injury (IP, 5/20 mg/kg; LPS-induced mouse model of ALI)	72
17		● **Affinity:** K_d = 210 nM (FP) ● **Cell:** reduction of ROS, NO, and TNF-α @10 μM (LPS-induced mouse peritoneal macrophages; EC_{50} ∼ 1 μM for NO and TNF-α) ● **DMPK/Tox:** solubility = 91.1/169.5 μg/mL (free/salt, pH 7); no cytotoxicity @100 μM over 24 h (Cell Titer Blue; mouse peritoneal macrophages); in vivo PK (rats): $t_{1/2}$ = 4.31/19.92 h and CL = 5.57/6503 mL/h/kg (IV/IG administration of 5/20 mg/kg) and F = 19.86% ● **In vivo pharmacology:** Nrf2 nuclear translocation and reduced cytokine levels (TNF-α, IL-1β, IL-6) in bronchoalveolar lavage fluid and lung tissue (IP, 5–20 mg/kg; LPS-induced mouse model of ALI)	73

TABLE 1 (CONTINUED)

#	Structure	●Affinity ●Cell activity ●DMPK/Tox ●*In vivo* pharmacology	Ref
18		● **Affinity:** K_i = 0.22 μM (FP) ● **Cell:** reduction of TNF-α, IL-6, ROS, and NO @10 μM (LPS-induced mouse peritoneal macrophages) ● **DMPK/Tox:** solubility = 404/484 μg/mL (free/salt, pH 7); no cytotoxicity @100 μM over 24 h (Cell Titer Blue; mouse peritoneal macrophages); *in vivo* PK (rats): $t_{1/2}$ = 12.74/5.75 h and CL = 3445/1906 mL/h/kg (IV/IP administration of 5/20 mg/kg) ● *In vivo* **pharmacology:** Nrf2 nuclear translocation, reduced cytokine levels (TNF-α, IL-1β, IL-6) in bronchoalveolar lavage fluid and lung tissue, and reduced lung injury (IP, 2.5–10 mg/kg; LPS-induced mouse model of ALI)	74
19		● **Affinity:** K_i = 940 nM (FP) ● **Cell:** ROS reduction, HO-1, NQO1, GPX4 rescue, total Nrf2 and nuclear expression increase, mitochondrial membrane potential (MMP) increase, p-Tau and BACE1 decrease, NDP56 and PSD95 increase, mEPSC frequency increase @20 μM (Aβ$_{1-42}$-treated primary cultured cortical neurons) ● **DMPK/Tox:** no cytotoxicity @1–100 μM (primary cultured cortical neurons); no obvious toxic effects on heart, liver, lung, spleen, or kidney (histology; 40 mg/kg/day for 60 days, APP/PS1 AD mice); *in vivo* PK (rats): $t_{1/2}$ = 2.75 h and CL = 2316 mL/h/kg (IV, 28 mg/kg), and F = 4.0 % (IG *vs* IV); brain permeability = 347.2 ± 160.3 ng/mL in tissue at 30 min (IG, 40 mg/kg; Aβ$_{1-42}$-induced AD mice) ● *In vivo* **pharmacology:** improved cognitive functions (spatial memory, novel object recognition, learning ability) and restored brain structure damage (40 mg/kg/day for 60 days; APP/PS1 AD mice); also observed in same mice: SOD and GSH recovery; Nrf2 translocation; increased Nrf2-ARE binding; increase of antioxidant enzymes (Nrf2, HO-1, NQO1, and GPX4); reduced AD biomarkers (Aβ, p-Tau) and increase of BACE1, NDP56, and PSD-95 in hippocampus and cortex.	75
20		● **Affinity:** IC$_{50}$ = 60 nM (FP); K_d = 102 nM (SPR) ● **Cell:** 2–3-fold increased Nrf2 nuclear translocation and downstream target activation @10 μM (Nrf2, NQO1, HMOX1, GCLM, GCLC) (6/24 h; HaCaT) ● **DMPK/Tox:** solubility = 380 μM; ∼100% left @20 min (mouse and human liver microsomes); diminished mutagenicity (mini-Ames w S9) compared with **8**	77
21		● **Affinity:** IC$_{50}$ = 73 nM (FP) ● **Cell:** 1.4–7-fold increased Nrf2 and NQO1 expression @1–10 μM (16 h; HaCaT); target engagement in cells (CETSA) @10 μM and increased Nrf2 levels @2.5/10 μM (HL-60); 2–8-fold upregulation of NQO1 activity @1–10 μM (Hepa1c1c7 and ARPE-19) ● **DMPK/Tox:** $logD_{7.4}$ = 0.5 (compared with -1.5 for **20**); $t_{1/2}$ = 136 min (human liver microsomes) ● *In vivo* **pharmacology:** 2.2–2.8-fold induction of NQO1 mRNA levels in mouse liver (PO, 10/25 mg/kg, four times, 24 h apart) (also effect on NQO1 protein in liver and mRNA in kidney @25 mg/kg); dose-dependent thermostabilization of Keap1 in mouse liver (PO, 10/25/50 mg/kg, four times, 24 h apart); 1.5–2-fold lower levels of ALT and AST (p = 0.0598 and 0.0176, respectively) in the APAP-induced hepatotoxicity model (PO, 25 mg/kg/day, 3 days; 24 h before APAP; C57BL/6 male mice)	78,79

TABLE 1 (*CONTINUED*)
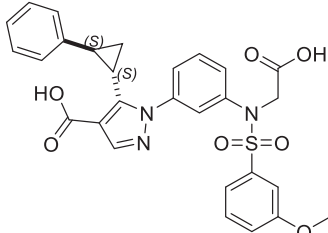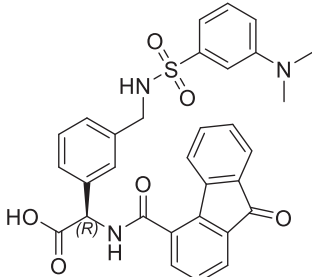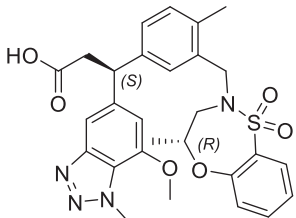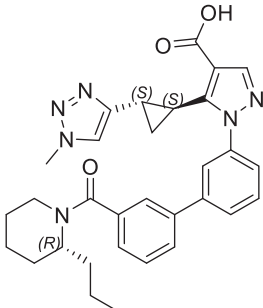
#	Structure	•Affinity •Cell activity •DMPK/Tox •*In vivo* pharmacology	Ref
22		• **Affinity:** IC_{50} = 151 nM (FP)	[80]
23	LH835	• **Affinity:** IC_{50} = 144 μM (FP) and 8.9 nM (TR-FRET) • **Cell:** fourfold induction @10 μM (ARE-luciferase reporter assay; HepG2-ARE-C8); 4–18-fold upregulation of NQO1 mRNA and 2–3-fold upregulation of HO-1 and NQO1 protein @5–10 μM (6–24 h; mouse BV-2 microglial cells); suppression of LPS-induced cytokines (IL-1β, IL-6, and TNF-α) @10 μM (24 h, LPS-stimulated mouse BV-2 microglial cells) • **DMPK/Tox:** no cytotoxicity @1–50 μM (HepG2 and BV-2 microglia)	[81]
24	LH945	• **Affinity:** IC_{50} = 150 nM (FP) • **DMPK/Tox:** 98% left @90 min (human liver microsomes)	[82]
25		• **Affinity:** IC_{50} = 0.575 μM (FP); K_d = 0.500 μM (ITC); ΔT_m = 3.3 °C @10 μM (differential scanning fluorimetry, DSF) • **Cell:** 1.5–2.5-fold increased NQO1 activity @10–100 μM (24 h, Hepa1c1c7) (CDDO-Me: threefold @0.1 μM, but cytotoxic at 1 μM); Up to threefold upregulation of Nrf2 target genes (NQO1, HMOX1, GSTP, GCLC, GCLM) @50 μM (Hepa1c1c7); potential target engagement in cell lysate @50 μM (CETSA) • **DMPK/Tox:** solubility = 348 μg/mL; no cytotoxicity @100 μM (ARPE19 cells) (SFN: Cytotox IC_{50} = 10 μM); $\log P_e$ = -5.17 (PAMPA)	[83]
26		• **Affinity:** IC_{50} = 0.45 μM (FP) • **Cell:** no upregulation of GSTM3, HMOX1, NQO1 @1–100 μM (NCM460D)	[84]

TABLE 1 (*CONTINUED*)

#	Structure	●Affinity ●Cell activity ●DMPK/Tox ●*In vivo* pharmacology	Ref
27		● **Affinity:** IC_{50} = 64.5 nM (FP); IC_{50} = 14.2 nM (TR-FRET) ● **Cell:** 2–15-fold upregulation of GSTM3, HMOX1, NQO1 mRNA @10–100 μM (NCM460D)	84,85
28	 K22	● **Affinity:** IC_{50} = 0.18 μM (FP) ● **Cell:** inhibition of Keap1-Nrf2 in coimmunoprecipitation assay @10 μM (H9c2 cell lysate); upregulation of Nrf2, HO-1, and NQO1 mRNA (2–9-fold) and protein (1.5–2.5-fold) @1–10 μM (4–16 h; H9c2); 10%–20% improvement in cell viability and decrease of IL-6, IL-1β, TNF-α, and ROS @1–10 μM (LPS-treated H9c2) ● **DMPK/Tox:** solubility = 16.38 μg/mL; 96% left@30 min (human liver microsomes); no cytotoxicity @3–50 μM (H9c2); no mutagenicity @1–100 μM (mini-Ames)	86
29		● **Affinity:** IC_{50} = 0.20 μM (FP); K_i = 2.1 nM (FP); K_d = 26 nM (SPR) ● **Cell:** 1.5–2.5-fold increase in NQO1 mRNA @20–100 μM (MEF cells) ● **DMPK/Tox:** 81% left @30 min (human liver microsomes); no cytotoxicity @50 μM (WST-8, HepG2 cells)	46,87
30		● **Affinity:** IC_{50} = 22 nM (FP); K_d = 58.4 nM (ITC); K_d = 26.4 nM (BLI) ● **Cell:** 2–8-fold induction @0.1–20 μM (ARE-luciferase reporter assay; HepG2) (SFN: 2–4-fold); upregulation of Nrf2, HO-1, NQO1, and GCLM mRNA (2–11-fold) and protein @0.1–10 μM (4–24 h; H9c2); 10%–30% improvement in cell viability, decrease of IL-6, IL-1β, TNF-α, and ROS, and upregulation of GSH/GSSG ratio @0.1–10 μM (LPS-treated H9c2) ● **DMPK/Tox:** 74.4% left @45 min and $t_{1/2}$ = 151 min (human liver microsomes); P_e = 5.27 × 10^{-6} cm/s (PAMPA); 9%–47% inhibition of main CYPs (1A2, 2C9, 2C19, 2D6, 3A4) @10 μM; $t_{1/2}$ = 4.02 h and CL = 0.11 L/h/kg (IV, 5 mg/kg); no cytotoxicity @3–100 μM (H9c2) ● *In vivo* **pharmacology:** ameliorated heart damage (histology), reduced inflammation (serum IL-6, IL-1β, TNF-α), activated Nrf2 pathway (Nrf2, HO-1, NQO1, GCLM), reduced ROS, and increased GSH/GSSG ratio (heart tissue) (IP, 10/40 mg/kg/day, 3 days, LPS-treated mice)	88
31	 Pro2	● **Affinity:** parent drug release (to the monoacidic analogue): >98% @3h with 10 mM H_2O_2 (HPLC); IC_{50} = 96.7 nM (FP) and K_i = 58.5 nM (ITC) of parent monoacidic compound ● **Cell:** uptake of prodrug and conversion to parent drug (macrophage RAW264.7 cells stimulated with H_2O_2 for 24 h); 2–11-fold induction and EC_{50} of 0.32 μM (ARE-luciferase reporter assay; LPS-stimulated ROS-producing HepG2-ARE-C8 cells); upregulation of Nrf2-controlled genes (7–13-fold, HO-1, NQO1, GCLM) and proteins, restoration of antioxidant capacity (SOD and GSH-Px activity, GSH/GSSG ratio, MPO activity), and reduction of cytokines (mRNA and protein; IL-6, IL-1β, TNF-α) @500 nM (LPS-treated RAW264.7 cells); EC_{50} = 0.12 μM (NO reduction; LPS-treated RAW264.7 cells)	89

TABLE 1 (CONTINUED)

#	Structure	●Affinity ●Cell activity ●DMPK/Tox ●*In vivo* pharmacology	Ref
		● **DMPK/Tox:** $logD_{pH7.4}$ = 2.34; solubility = 879.6 µg/mL; P_e = 6.35 × 10^{-6} cm/s (PAMPA); *in vivo* PK (rats): $t_{1/2}$ = 2.09 h (PO, 10 mg/kg), F = 68.1%; stability studies: >60% left @24 h (PBS, pH = 4–10), >50% left @8h (simulated gastric and intestinal fluid), >90% left @12 h (rat plasma) and @45 min (rat liver microsomes) ● ***In vivo* pharmacology:** diminished levels of proinflammatory cytokines (serum IL-6, IL-1β, TNF-α and IFN-γ) (IG, 10/40 mg/kg/day, 3 days, LPS-treated female C57BL/6 mice)	

Keap1 inhibitors found by FBDD

#	Structure	●Affinity ●Cell activity ●DMPK/Tox ●*In vivo* pharmacology	Ref
32		● **Affinity:** K_i = 40 nM (FP) ● **Cell:** not active ● **DMPK/Tox:** P_e = 0.9 nm/s (PAMPA); $t_{1/2}$ > 4 h (mouse liver microsomes), >3h (human blood plasma)	35
33		● **Affinity:** K_i = 280 nM (FP) ● **Cell:** <2-fold upregulation of HO-1, NQO1, and TRXR1 (mRNA and protein) @200 µM (HaCaT); Nrf2 dependent; less potent than 4-OI and an analogue of **36** ● **DMPK/Tox:** no cytotoxicity (200 µM; HaCaT)	45
34	KI-696	● **Affinity:** 95% @15 nM (FP); K_d = 1.3 nM (ITC); K_d = 1.4 nM (SPR) ● **Cell:** nuclear Nrf2 translocation @0.01–10 µM (NHBE); increase in NQO1 and GCLM mRNA levels and NQO1 activity @1 µM to the same level as 100 nM CDDO-Me (NHBE); EC_{50} = 12 nM (NQO1 activity; BEAS-2B); EC_{50} = 16–36 nM (5–10-fold upregulation of NQO1, GCLM, HO-1, TXNRD1 mRNA; COPD patient epithelial cells); 2.5–fold NQO1 induction @1–10 µM (Hepa1c1c7) ● **DMPK/Tox:** F = 7% and CL = 70 mL/min/kg (rat); no cytotoxicity (10 µM; BEAS-2B); no/low activity in a panel of 49 toxicity targets ● ***In vivo* pharmacology:** EC_{50} = 26–44 µmol/kg (9–37-fold upregulation of NQO1, HO-1, TXNRD1, SRXN1, GSTA3, GCLC mRNA in lungs; 6 h IV infusion; rats); fewer immune cells in lung fluid and more GSH in lung tissue (6 h IV infusion of 35 µmol/kg; rat ozone model of COPD)	34,46
35		● **Affinity:** IC_{50} < 15 nM (FP); K_d = 2.5 nM (SPR) ● **Cell:** EC_{50} = 43 nM (BEAS-2B NQO1 MTT assay); ~10–30-fold upregulation of NQO1, GCLM, TXNRD1 mRNA @50–100 nM; NHBE cells) ● **DMPK/Tox:** chrom $logD_{7.4}$ = 3.0; P_e = 16 nm/s (AMPA)	91

TABLE 1 (CONTINUED)
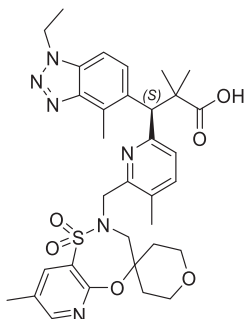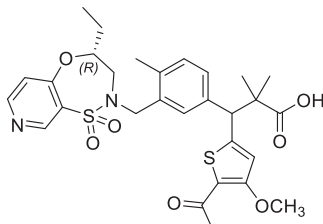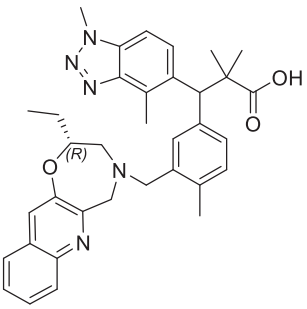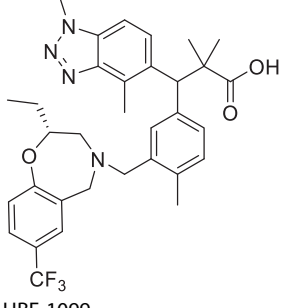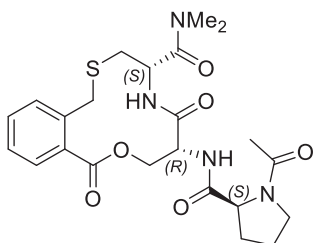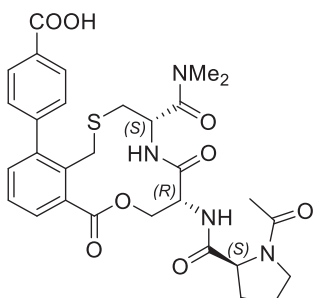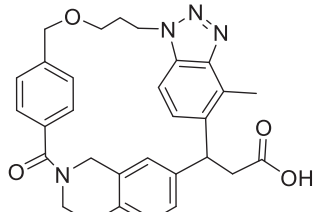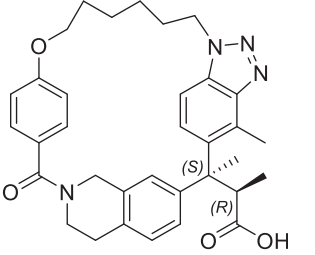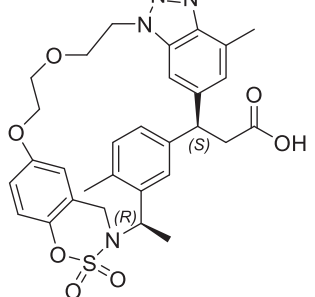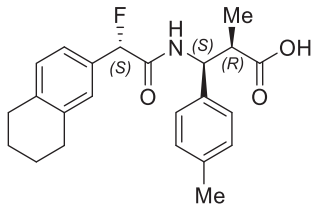
#	Structure	•Affinity •Cell activity •DMPK/Tox •*In vivo* pharmacology	Ref
36		• **Affinity:** K_d < 1 nM (TSA) • **Cell:** EC$_{50}$ = 0.56 nM (ARE-luciferase reporter assay; HEK293)	93
37		• **Cell:** IC$_{50}$ = 0.19 nM (bioluminescence resonance energy transfer; HCE-T); EC$_{50}$ = 2.98 nM (ARE-luciferase reporter assay; HCE-T) • **DMPK/Tox:** 48% left @30 min (human liver microsomes)	94
38		• **Affinity:** K_d < 100 nM (FP) • **Cell:** 1.5-fold upregulation of NQO1 @0.5 nM (Hepa1c1c7)	95
39	 UBE-1099	• **Affinity:** IC$_{50}$ = 47 nM (FP) • **DMPK/Tox:** ~1–30 μM of compound in plasma at 1–24 hours after a 30 mg/kg dose (PO; BALB/c mice); no noticeable toxicity and no effect on heart rate, blood pressure, food intake, or muscle weight (PO, 30 mg/kg/day, for up to 16 weeks; Alport mice); no effect on endothelin expression @10–100 nM (as seen for CDDO-Im; rat proximal tubule cells) • ***In vivo* pharmacology:** 5–9-fold induction of NQO1 mRNA in kidney after 14 h after a 3/30 mg/kg dose (2–4-fold seen for CDDO-Im; PO; BALB/c mice); reduced mRNA plasma creatinine, blood urea nitrogen (BUN), and renal injury marker (lipocalin-2); 30% of glomeruli with severe glomerulosclerosis (50% for vehicle), suppression of macrophage infiltration and fibrosis in kidney, downregulation of inflammatory cytokine genes (Mcp1, IL-β, IL-6, TNF-α), fibrosis genes (Tgf-β, Mmp9), and kidney-injury marker (Kim1), increased kidney expression of Nrf2 and NQO1 (PO, 30 mg/kg/day, week 22 Alport mice); median survival time increased from 210 to 250 days (30 mg/kg/day; Alport mice)	96
Macrocycles 40		• **Affinity:** K_d = 4.1 μM (SPR, in solution); K_d = 3.7 μM (ITC) • **Cell:** 40% @256 μM (Nrf2 nuclear translocation assay; U2OS cells) • **DMPK/Tox:** CL$_{int}$(human microsomes) = 36.5 μL/min/mg; aqueous solubility = 805 μM; P$_{app}$(A-B) = 1.6 × 10^{-6} cm/s (Caco-2 incl. efflux pump inhibitors)	99

TABLE 1 (CONTINUED)

#	Structure	•Affinity •Cell activity •DMPK/Tox •*In vivo* pharmacology	Ref
41		• **Affinity:** K_d = 41 nM (SPR, in solution); K_d = 68 nM (ITC) • **Cell:** 16% @256 µM (Nrf2 nuclear translocation assay; U2OS cells) • **DMPK/Tox:** CL_{int}(human microsomes) < 3 µL/min/mg; aqueous solubility > 805 µM; P_{app}(A-B) = 0.16 × 10^{-6} cm/s (Caco-2 incl. efflux pump inhibitors); High selectivity (EC_{50}/IC_{50} > 100 µM) over 88 potential off-targets (CEREP panel)	[100]
42		• **Affinity:** 100% inhibition @100 nM (TR-FRET) • ***In vivo* pharmacology:** 6.5- and 22-fold upregulation of NQO1 mRNA in kidney and liver, respectively (3 mg/kg, PO, rats) (a nondisclosed compound called SCO-116 improves kidney function in CKD and ameliorates NASH in mice; 1 mg/kg/day, PO)	[101]
43		• **Affinity:** IC_{50} = 1.6 nM (TR-FRET) • **Cell:** EC_{50} < 1 nM (BEAS-2B NQO1 MTT assay); EC_{50} = 38 nM (upregulation of human gamma-globin mRNA; HUDEP)	[102]
44	 S217879	• **Affinity:** K_d = 4.15 nM (SPR) • **Cell:** EC_{50} = 23 nM (Nrf2 nuclear translocation assay; U2OS cells); EC_{50} = 18 nM (ARE-reporter assay; HepG2 cells); reduce H_2O_2-stimulated ROS production in HepG2 @1 mM; EC_{50} = 16 nM (upregulation of NQO1 mRNA; primary hPBMCs); inhibition of IL-1β and MCP1 secretion (LPS-stimulated hPBMCs) @30/100–1000 nM • **DMPK/Tox:** no activity against 110 potential off-targets (CEREP safety panel) @10 µM; P_{app}(A-B) = 4.5 × 10^{-6} cm/s and efflux ratio = 4.5 (Caco-2); solubility > 100 µM; IC_{50} = 5 µM and 18 µM (CYP2C8 and 2C9 inhibition); CYP phenotyping (>95% 3C4); CL_{int} (mL/min/g prot) in microsomes/hepatocytes/ hepatocytes + plasma = 226/340/87 (mouse), 22/130/58 (rat), 122/244/15 (dog), 243/940/179 (cyno), and 35/106 /21 (human); *in vivo* PK (C57BL/6 male mice): 30 mg/kg PO led to C_{max} 3.2 µM and AUC of 3.8 µM*h, $t_{1/2}$ ∼ 30–45 min; 10% hERG inhibition @10 µM; 17% Nav1.5 inhibition human @10 µM; LD_{50} > 30 µM (HepG2); no impact on cell proliferation @10 µM (HepG2), no AKT phosphorylation @10 µM (hepatocytes and HepG2); no major toxicity (non-GLP dose range finding in rats and nonhuman primates), but hepatocellular hypertrophy seen in rodents; upregulation of Nrf2 target genes, antisteatotic effects, reduced oxidative stress, DNA damage, apoptosis and inflammation, and inhibition of fibrogenesis @3 µM (2 days; patient-derived liver slices) • ***In vivo* pharmacology:** 2–12-fold upregulation of mRNA NQO1, GCLC, GSTM1, and GPX2 in liver @30 mg/kg at 4–24 after administration (PO, single dose or chronic administration; C57BL/6 male mice); reduction in NAS, reduction of liver triglycerides, upregulation of antioxidant genes (NQO1, GPX2) and downregulation of proinflammatory genes (CCL5, CD68, IL-1β, IL-6) in liver, and increase in liver weight (PO, 30 mg/kg/day for 2 weeks; MCDD model); reduction in NAS, no	[103–105]

TABLE 1 (CONTINUED)

#	Structure	•Affinity •Cell activity •DMPK/Tox •In vivo pharmacology	Ref
		change in food intake or body weight, increased liver weight, reduction in liver triglycerides, reduction of fibrosis and stellate cell activation, upregulation of antioxidant genes (NQO1, GSTM1, GCLC, GPX2), reduction in inflammatory response and genes (PO, 30 mg/kg/day for 8 weeks; DIO NASH model).	
Others 45		• **Affinity:** IC_{50} = 0.089 μM (SPR, competition); K_d = 0.130 μM (ITC) • **Cell:** twofold increase of HO-1 @2 μM (human renal mesangial cells, HRMCs; twofold induction seen for 10 μM of compound **1** as control) • **DMPK/Tox:** solubility (FaSSIF and FeSSIF) ≥ 475 and 303 μM; P_{app}(A-B) = 33 × 10^{-6} cm/s (Caco-2); 70% and 87% left @1h (human and rat liver microsomes); in vivo PK (male CD rats): 1 mg/kg IV led to $t_{1/2}$ = 4.5 h and CL_{tot} = 0.03 L/h/kg; 3 mg/kg PO led to C_{max} = 25.7 μM and AUC = 324 μM*h; F = 136% • **In vivo** pharmacology: 4.6-fold increased expression of HO-1 in kidney after 6 h (PO, 30 mg/kg; Wistar rats)	106

1,4-Diaminonaphthalenes and analogues

The most studied scaffold in this area is probably the 1,4-diaminonaphthalene core. The first compound was discovered in 2013 by Marcotte et al. by HTS of about 270,000 compounds using a homogeneous confocal fluorescence anisotropy (2D-FIDA) assay.[59] Compound **7**, belonging to the benzenesulfonamide para-substituted subclass, showed an IC_{50} of 2.7 μM. Later an IC_{50} value of 1.46 μM (FP) and K_d of 1.69 μM (biolayer interferometry, BLI) were determined.[60] In an ARE reporter cell assay, sevenfold induction of luciferase was observed for **7** at 100 μM, but there was no effect at 30 μM. In comparison, DMF gave six- and eightfold induction at 30 and 100 μM, respectively. Additionally, **7** increased Nrf2 and NQO1 protein levels in an Nrf2-dependent manner.[59] These findings spurred an explosion of new analogues in the subsequent years in the search for improved potency and druglikeness. Jiang et al. reported a structure-based approach, pointing out that occupation of the P1 and P2 subpockets of Keap1 (Figure 3) by the carboxyl groups of Nrf2 is key for the design of new inhibitors.[60] Thus, starting from **7**, they developed the first inhibitor, compound **8** (CPUY192002), with low nanomolar affinity by linking two aliphatic carboxylic acid chains to the sulfonamide groups. The activation of the Nrf2-ARE system (up to 15.3-fold, similar to sulforaphane, SFN) and the increased expression of Nrf2-regulated cytoprotective genes further confirmed the promising role of compound **8** and its potential to guide the design of new derivatives. Interestingly, the peak time of the increased gene expression was 16–32 h, which was delayed and prolonged compared with covalent inhibitors (6–8 h).[60]

The SAR around **7** and **8** was initially investigated by Jain et al. through extensive substitution patterns in the benzenesulfonyl moiety and naphthalene region and replacement of the N-acetic acid portions.[61] Optimal potencies were obtained by 1,4-substitution on the naphthalene core and electron-donating groups in the meta or para position of the benzene moiety. However, the most interesting result was obtained for the N-diacetamide analogue **9**, with similar in vitro activity to **8**. Since good activity was also obtained by the corresponding monocarboxylic acid analogue (IC_{50} = 61 nM by FP; K_d = 110 nM by SPR), the authors implied that the diacetic acid portions are not essential for obtaining Keap1-Nrf2 inhibition.

Subsequent optimization focused on the limited solubility of **8**. The physiochemical effects of different substituents on the benzenesulfonyl groups were systematically evaluated taking both electron-donating and electron-withdrawing moieties into account.[62] This revealed p-acetamido compound **10** (CPUY192018) as the best candidate. It showed the best trade-off between affinity (IC_{50} = 14.4 nM by FP[62]; K_d = 39.8 nM by isothermal titration calorimetry, ITC[63]) and solubility, together with increased expression of Nrf2 downstream proteins (NQO1, HO-1, GCS) in cells and a reduction of proinflammatory cytokines (TNF-α, IFN-γ, IL-6, IL-12 and IL-17) in lipopolysaccharide (LPS)-challenged mice.[62] The encouraging results of compound **10** prompted further evaluation in different inflammatory disease models. Lu et al. proved its therapeutic potential in both ulcerative colitis (UC) and renal inflammation.[63,64] The cytoprotective effect was initially investigated in NCM460 colonic cells, where **10** increased nuclear Nrf2 translocation, elevated the expression of Nrf2 target genes (HO-1, GCLM, GPx2), and protected cells against dextran sodium sulfate (DSS)-induced oxidative injury in a concentration-dependent manner owing to the reduction of ROS levels. Inflammation and oxidative stress in the colon were similarly reduced in an in vivo mouse model of chronic UC, since the administration of **10** (10 or 40 mg/kg/day) for 64 days attenuated body weight loss, rectal bleeding, and shortening of the colon length, and preserved histological

colonic structure. Additionally, levels of inflammatory cytokines (TNF-α, IFN-γ, IL-6, IL-1β) and myeloperoxidase (MPO) activity were reduced in the colon, as were ROS levels.[63]

Later, compound **10** was identified as a potential treatment option for chronic kidney inflammation. The effects in the HK-2 cell line (human proximal tubular epithelial cells) confirmed the ability to impair ubiquitin-mediated degradation of Nrf2, upregulate the Nrf2-ARE-controlled cytoprotective genes HO-1, NQO1 and GCLM by 5–7-fold, increase the activity of antioxidant enzymes, i.e. superoxide dismutase (SOD), catalase (CAT), and glutathione peroxidase (GPx), protect against LPS-induced cytotoxicity (reflected by restoration of cell viability), inhibit NF-κB activation, and suppress inflammatory factors (TNF-α, IL-18, IL-1β, IL-6 and nitric oxide [NO]). Kidneys from mice with LPS-induced chronic renal inflammation showed the same benefits encountered *in vitro*, with compound **10** alleviating oxidative stress injuries and pathological alterations in renal structure and function.[64] In the same year, Hui *et al.* investigated the protection of compound **10** in retinal ischemia–reperfusion (I/R) injury, one of the major causes of visual loss. Using a virtual optomotor system that allows the quantitative assessment of spatial vision, the authors determined a strong therapeutic effect on visual function in rodents. Both systemic (10 mg/kg) and topical (1 mg/kg) administration of **10** conferred Nrf2 target gene activation in the retina, similarly to that induced by CDDO-Me (1.5 mg/kg).[65] Compound **10** was further tested in COPD models. Its therapeutic effects were ascribed to a dose-dependent increase in Nrf2 nuclear translocation and related gene expression (HO-1, NQO1 and GST), reduction of basal glycolysis by disruption of the Keap1-actin interaction, and enhanced phagocytosis of *Haemophilus influenzae* and *Streptococcus pneumoniae* with 10 μM of compound **10** in COPD mice alveolar macrophages. These findings demonstrated for the first time the ability to simultaneously interfere with the Keap1-Nrf2 protein–protein interaction (PPI) to counteract oxidative stress and the Keap1-actin PPI to reprogram metabolism. Identical effects on metabolism and phagocytosis were obtained in alveolar macrophages from cigarette smoke condensate (CSC)-induced COPD mice where compound **10** also inhibited the production of plasma inflammatory cytokines (TNF-α, IFN-γ, IL-5, IL-6).[66]

In search of optimized analogues of compound **10**, the replacement of the diacetic moiety with various bioisosteric substituents (such as nitrile, alkyne, esters, amide, alcohols and triazole groups) led to a new family of derivatives, among which only compound **11**, bearing tetrazole groups, did not suffer a drastic decrease in activity. It showed improved physiochemical properties and membrane permeability compared with **10**, and it was more efficacious in upregulating Nrf2-driven genes and proteins.[67]

In the last few years, many research groups have worked on the 1,4-diaminonaphthalene scaffold, varying both the benzenesulfonamide moiety and the naphthalene core itself. One of the first asymmetric 1,4-diaminonaphthalene analogues is the pyrrolidine compound **12** (RA839) found during screening in 2015 by Sanofi.[68] The compound induced expression of ARE-driven genes and Nrf2 nuclear translocation in cells, and significantly changed the expression of 105 genetic probe sets in bone marrow-derived macrophages (BMDMs) in a highly Nrf2-dependent manner. Furthermore, **12** reduced NO release and the expression of NO synthase 2 (NOS2) mRNA, while stimulating expression of NQO1 in LPS-stimulated BMDM. The compound was inactive in an off-target panel but was highly metabolically unstable. Accordingly, hepatic mRNA levels of Nrf2 target genes were detected in mice 3 h after administration, but only with concomitant reduction of oxidative hepatic metabolism using a cytochrome P450 inhibitor.

Lu *et al.* recently reported two other families of promising asymmetric Keap1-Nrf2 inhibitors. First, they explored a range of amino acids as substituents to the naphthalene core instead of one of the *N*-acetic acid-substituted benzensulfonamide moieties.[69] Most of the 40 new derivatives bearing aliphatic, polar, or aromatic amino acids had poor activity, but the proline derivative **13** showed an impressive IC$_{50}$ value of 43 nM in FP assay and similar affinities by biophysical methods. Substituting the benzene with paramethyl or three methyl groups instead of methoxy led to > 100-fold loss in affinity, demonstrating a narrow SAR. Compound **13** showed target engagement in hepatic L02 cells by the cellular thermal shift assay (CETSA) and activated the Nrf2-controlled cytoprotective defense system. Moreover, prevention of acetaminophen (APAP)-induced apoptosis and reduction of hepatic injury markers with no apparent cytotoxicity were detected in L02 cells. Inflammatory and pathological signals in APAP-challenged mice were similarly relieved by a single 10 mg/kg pretreatment with compound **13**.[69] Another set of structural variations led to the 2-oxy-2-phenylacetic acid-substituted naphthalene sulfonamide derivative **14**, with strong binding affinity to Keap1 Kelch.[70] Antioxidant and antiinflammatory capacities were demonstrated in an LPS-treated macrophage cell line (RAW264.7) by reduced ROS generation, activation of the Nrf2-ARE pathway and restoration of the GSH/GSSG ratio. In LPS-treated mice, an IP injection of **14** diminished the serum levels of IFN-γ, IL-1b, IL-6 and TNF-α. Furthermore, the compound was stable in rat liver microsomes.[70]

Sun *et al.* reported the aniline-based derivative **15** (NXPZ-2), which exhibited Nrf2-dependent neuroprotective activity in an Alzheimer's disease (AD) mouse model, with improvement in learning and memory function and a concomitant increase of Nrf2 nuclear translocation, Nrf2-targeted antioxidant enzymes (HO-1, NQO-1), and hippocampal/cortical SOD and GSH. Additionally, a significant decrease of p-Tau and Aβ$_{1-42}$ serum levels was observed, and **15** did not show toxicity in neurons or mice organs (heart, liver, and kidney).[71] The promising results for compound **15** prompted several follow-up designs. A molecular hybridization of **15** and SFN led to the sulfoxide derivative **16** (SCN-16), with more potent antioxidative and antiinflammatory activity than **15** in LPS-treated mouse peritoneal macrophages and reduced lung injuries in the LPS-induced mouse model of acute lung injury (ALI).[72] Additionally, crystallography-guided optimization led to the asymmetric piperazinyl-derivative **17**, which showed better solubility than **15** and similar effectiveness in suppressing NO and cytokine levels in LPS-treated mouse peritoneal macrophages and the ALI mouse model.[73] Likewise, the (*R*)-azetidine derivative of **15**, compound **18**, displayed improved solubility compared with **15** (and **17**) and similar inhibitory activity by FP, as well as antioxidant and antiinflammatory effects in mouse peritoneal macrophages. Furthermore, *in vivo*

efficacy was proven in LPS-induced ALI mice as **18** decreased proinflammatory cytokines, induced Nrf2 nuclear translocation, and alleviated pathological features (infiltrations, bleeding, congestion) in lung tissue.[74] Finally, the phosphodiester analogue **19** (POZL) was recently presented as a promising candidate for treating AD.[75] Long-term oral treatment of transgenic APP/PS1 AD mice improved their cognitive functions and restored brain structure damage without causing toxic effects in organs. Furthermore, activation of the Keap1-Nrf2 pathway and positive effects on AD biomarkers were confirmed in the transgenic mice and cortical neurons.[75]

To avoid potential metabolic reactivity of naphthalenes (reactive oxides or naphthoquinones),[76] many efforts have been devoted to alternative scaffolds, such as nitrogen-containing heterocycles (pyridine, quinoline, indole, phthalazine) and benzenes. Initially, the poor potency and solubility of nonfused ring systems confirmed the necessity of a 6,6-fused framework to afford valuable inhibitors.[77] Hence, 1,4-isoquinoline **20** emerged as the best candidate, displaying high inhibitory potency by FP and affinity to Keap1 Kelch by SPR. Additionally, Nrf2 stabilization and downstream target activation in immortalized human keratinocytes (HaCaT cells) were observed, and **20** showed good metabolic stability in liver microsomes and high aqueous solubility. Through a mini-Ames assay, an improved mutagenicity profile compared with naphthalene **8** was further demonstrated.[77] However, the negative logD$_{7.4}$ value (-1.7) and the two negatively charged carboxylic groups of **20** were noted as likely causes of low membrane permeability, which prompted the replacement of one carboxylate with an electron-withdrawing and lipophilic portion. Following up on these findings led to a variety of fluoroalkylated analogues, where the 2,2,2-trifluoroethyl monoacid isoquinoline compound **21** showed the greatest lipophilicity while also maintaining nanomolar potency and metabolic stability.[78]

Further biological studies of **21** revealed target engagement of **21** with Keap1, as demonstrated by CETSA in cell lysates and live cells (human promyelotic leukemia HL-60 cells), where the compound also increased Nrf2 levels.[79] Moreover, **21** increased the activity of NQO1 in murine hepatoma (Hepa1c1c7) cells and human adult retinal pigment epithelial cells (ARPE-19), with a similar effect and potency to SFN. A series of oral administrations of **21** increased NQO1 mRNA and protein levels in mouse liver and induced thermostabilization of Keap1. However, the effects were mainly limited to the liver; only minor effects on mRNA in kidney were seen, and there were no differences in brains, colons or lungs. Finally, in the APAP-induced hepatotoxicity mouse model, **21** decreased the levels of alanine aminotransferase (ALT) and aspartate aminotransferase (AST), thus indicating a hepatoprotective effect.[79]

Detailed SAR analysis of naphthalene-based inhibitors continued in recent works by Lazzara et al. and Abed et al. Previously, it was shown that the monoacidic analogue of **8** was quite potent in the FP assay (K_i = 61 nM).[61] This was exploited in the design of a series of monosulfonamide, phenethyl, and sulfone derivatives of compound **8**. Most compounds showed an activity drop, but reasonable affinity was observed for the sulfonamide-sulfone compound **22**, where the extra methyl group on the acid linker was responsible for a fivefold increase in affinity.[80] Abed et al.

developed a new series of aryl sulfonamide analogues, among which the oxygen-containing rings had enhanced inhibitory effects. In particular, the chloro-benzodioxane derivative **23** (LH835) showed potent inhibition of Keap1-Nrf2, an ARE-inducing activity higher than SFN and reference compound **8**, upregulation of Nrf2 target proteins (HO-1, NQO1) by two- and threefold (less so than SFN), and suppression of LPS-induced cytokines in cells.[81]

Newer design approaches have investigated the replacement of the naphthalene core with xylylene or phenyl groups. Xylylenes showed activities in the high nanomolar range, with the most potent example, compound **24**, also showing high metabolic stability.[82] Georgakopoulos et al. reported a series of phenyl bis-sulfonamide inhibitors and evaluated the influence of different substitutions in position 2 of the central phenyl ring.[83] Introducing a 2-benzyloxy portion, as in **25**, induced submicromolar affinity, aqueous solubility of 348 μg/mL, and the expression of Nrf2 target genes in cells. No cytotoxic effects were detected, in contrast to CDDO-Me and SFN. However, the low permeability of this series in PAMPA assay, due to the presence of the two ionizable carboxylate groups, could be a focus for future optimization.[83] A parallel exploration of benzene derivatives with varying O-linked aromatic rings at C2-position gave the 4-fluorobenzyl-substituted compound **26**, also with submicromolar affinity in FP assay but no activity in cells. However, the naphthalene version of this compound (**27**) showed increased lipophilicity, affinity, and cell activity.[84] Further expansion of this design strategy was recently presented.[85] In an attempt to mimic the conjugation system of naphthalene with a single-ring core, benzene modifications by Sun et al. led to the potent tetramethyl analogue **28** (K22), endowed with cytoprotective and antiinflammatory effects in a cardiomyocyte cell line.[86] Furthermore, high metabolic stability in human liver microsomes, no cytotoxicity, and no mutagenicity toward Salmonella typhimurium implied a good balance between inhibitory and metabolic properties.

Yasuda et al. discovered the Keap1-Nrf2 PPI inhibitor **29**, containing a benzo[g]indole core and an indole-3-hydroxamic acid portion.[87] It showed high inhibitory activity by FP, as confirmed in our validation study,[46] increased NQO1 mRNA levels in MEF cells at 100 μM (comparable to that of 10 μM tBHQ), metabolic stability in human liver microsomes, and a lack of cytotoxicity in HepG2 cells.

The effects of an indoline core instead of a naphthalene scaffold, along with the replacement of diacetate moieties by acyl sulfonamides, were then investigated. Among several derivatives, compound **30** showed high affinity toward Keap1 Kelch and antioxidant and cardioprotective effects both in vitro and in vivo. In particular, transcription of Nrf2-related genes (Nrf2, HO-1, NQO1, GCLM), a decrease of inflammatory factors (ROS, cytokines), and upregulation of the GSH/GSSG ratio were observed in LPS-treated H9c2 cells in a concentration-dependent manner (0.1–10 μM), without any apparent cytotoxicity. The above protective effects of **30** against LPS-induced heart injury were also confirmed in vivo.[88]

Finally, an innovative ROS-cleavable prodrug strategy was developed to improve the poor permeability caused by the carboxyl groups and to provide selective Nrf2 activation in tissues

and cells undergoing oxidative stress.[89] This was achieved by shielding the carboxylate group with a thiazolidinone moiety that confers stability and permeability under physiological conditions until reaction with H_2O_2 from the oxidative environment, whereby the parent compound is released. First, a double thiazolidinone analogue of **8** was observed to be only partially cleaved in H_2O_2 even after 12 hours. Instead, **31** was synthesized by coupling the thiazolidine moiety to the monoacidic analogue of **8**, which was shown by FP and ITC to bind Keap1 Kelch with high affinity. This prodrug was fully converted to the parent compound after 3 h in the presence of H_2O_2 (10 mM) in buffer and by macrophages (RAW264.7) stimulated to produce H_2O_2. Prodrug **31** also demonstrated high metabolic stability (in simulated gastric fluid and intestinal fluid, rat plasma, and liver microsomes) and improved membrane permeability compared with the parent compound. Activation of the Nrf2-ARE pathway was obtained in HepG2 cells only when they were stimulated by LPS to produce ROS. Likewise, in LPS-treated macrophages, **31** potently upregulated Nrf2-targeted genes, enhanced the antioxidant capacity, and reduced the production of proinflammatory cytokines. Finally, *in vivo* efficacy in LPS-induced mice confirmed the potential of Keap1 prodrug inhibitors in the treatment of chronic inflammatory diseases.[89]

Keap1 inhibitors identified by fragment-based drug discovery (FBDD)

Several Keap1 inhibitors have been developed by FBDD. Using a deconstruction–reconstruction approach, we developed **32**. Metabolic stability was good but membrane permeability and cell activity were low, probably because of the high polarity of the compound.[35] Instead, screening 2500 fragments using orthogonal biophysical assays, followed by SBDD, led to a series of fluorenone-based compounds showing medium–high affinity.[45] Compound **33** upregulated several Nrf2-controlled genes in a human keratinocyte cell line in an Nrf2-dependent manner without causing cytotoxicity, albeit at a relatively high concentration (200 µM) and less potently than the covalent Nrf2 activator 4-octyl-itaconate.

Astex Pharmaceuticals and GlaxoSmithKline (GSK) Pharmaceuticals have collaborated to develop some of the most potent and biologically active Keap1-Nrf2 inhibitors.[34,90,91] Screening 330 fragments by X-ray crystallography and SBDD, starting with phenylpropanoic acid as an 'anchor fragment' and growing into adjacent subpockets, gave **34** (KI-696), which binds to Keap1 Kelch with a very high affinity,[34,90] as also confirmed by our group.[46] Compound **34** potently activated the Nrf2 pathway in normal human bronchial epithelial (NHBE) cells, a human lung epithelial cell line (BEAS-2B), and cells derived from COPD patients. The compound showed only minor activities in an *in vitro* panel of functional assays related to toxicity liabilities.[34] Oral bioavailability in rats was low, but IV infusion led to the expression of Nrf2-regulated genes in lung tissue, attenuation of ozone-induced pulmonary inflammation, and less depletion of lung GSH levels.[34] Subsequently, **34** was shown to reverse defects of alveolar macrophages isolated from COPD patients in phagocytosis of *H. influenzae* and *S. Pneumoniae*.[92] Astex and GSK have also provided the highly potent phenylpyrazole com-

pounds,[91] as represented by **35**. This series was developed after searching their compound collection for aromatic carboxylic acid-containing scaffolds as starting points. Noticeably, physicochemical properties like TPSA and $logD_{7.4}$ needed to be carefully balanced to obtain membrane permeability and hence cell activity. An analogue of **35** has been tested and verified by us to bind with very high affinity to Keap1 Kelch and exhibits good membrane permeability and cellular activity. However, it has relatively low stability in mouse liver microsomes.[35,45,46]

Recently, several analogue series of **34** have been presented. Janssen Pharmaceuticals showed 665 examples, many of which, such as compound **36**, were highly potent in a protein-based thermal shift assay (TSA) and cells.[93] Senju Pharmaceutical Co., Ltd. focused on replacing the benzotriazole group with other aromatic heterocycles, and this also gave several cell potent compounds, such as **37**.[94] Ube Industries, Ltd. expanded the aromatic region at the oxazepine moiety and modified the sulfonamide part, leading to high-affinity Keap1-Nrf2 inhibitors exemplified by **38**.[95] Similarly, Ube Industries together with academic scientists presented compound **39** (UBE-1099) as a high-affinity and orally available Keap1-Nrf2 inhibitor with effects in Alport syndrome mice.[96] The compound ameliorated glomerulosclerosis, renal tissue inflammation, and fibrosis, and prolonged the lifespan without noticeable toxicity. Furthermore, transcriptome analysis revealed effects on Nrf2 signaling, the cell cycle, the cytoskeleton, and mitochondria genes after treatment.

Macrocycles

Macrocycles can have several advantages, such as enhanced binding affinity, improved selectivity, better membrane permeability, enhanced ADME properties, and even superior CNS availability.[97] They also provide good chances for difficult targets that have large, flat, and featureless binding pockets, such as PPIs.[98] For Keap1, several macrocycles have been developed recently.
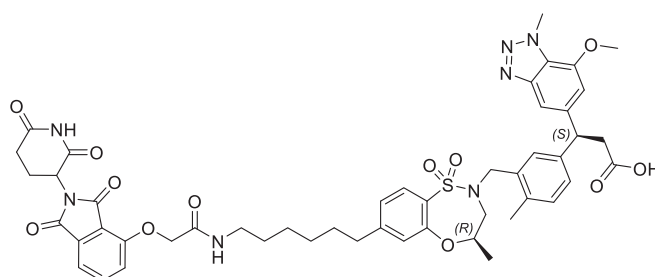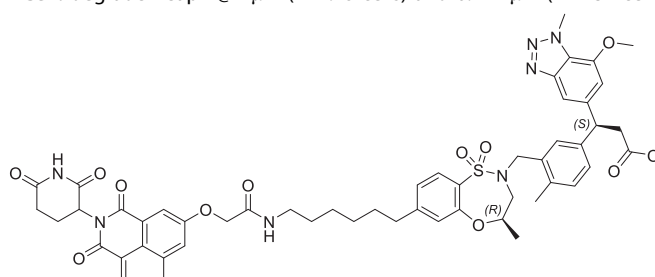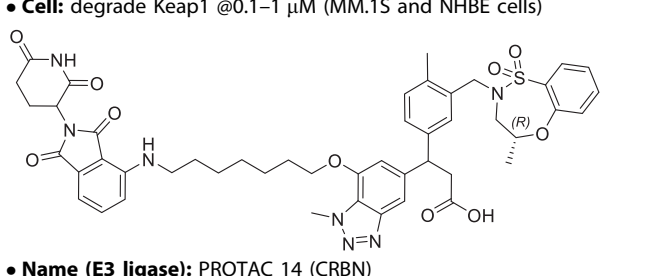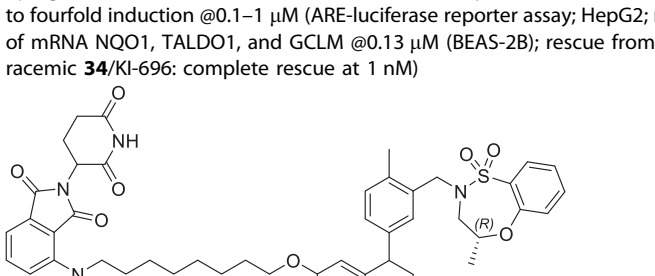
An *in silico* screening of a natural product library followed by structure-based optimization gave compound **40** with moderate binding affinity to Keap1, reasonable permeability across Caco-2 cell monolayers, and weak cell activity.[99] Follow-up research generated compound **41** with about 100-fold improved affinity but lower cellular potency and membrane permeability, likely as a consequence of introducing the carboxylic moiety.[100]

Scohia Pharma published 68 benzotriazole-substituted THIQ-based macrocycles in a patent application. Compound **42** achieved 100% Keap1-Nrf2 inhibition at 100 nM in a TR-FRET assay. After oral administration of 3 mg/kg to rats, NQO1 mRNA levels were increased 6.5- and 22-fold in kidney and liver, respectively.[101] Interestingly, the company webpage discloses data of a Keap1-Nrf2 inhibitor named SCO-116, which improves renal function and reduces fibrosis in mouse models of CKD and non-alcoholic steatohepatitis (NASH), respectively, after daily oral treatments of 1 mg/kg. Sanofi later presented 440 macrocycles that were structurally quite similar to Schohia's but had a wider range of variations. These also showed very high affinity in TR-FRET and nanomolar potency in cell assays, as exemplified by compound **43**.[102]

Recently, researchers from Servier designed a novel series of benzoxathiazine macrocycles from the X-ray structures of **34**

TABLE 2

Activities of Keap1-targeting PROTACs.

#	•Structure •Name (E3 ligase) •Affinity •Cell activity •DMPK/Tox • *In vivo* pharmacology	Ref
46	• **Name (E3 ligase):** NJH-04–086 (CRBN) • **Affinity:** IC$_{50}$ = 0.039 µM to Keap1 (TR-FRET) • **Cell:** degrade Keap1 @1 µM (MM.1S cells) and 0.1–1 µM (IMR-32 cells)	113
47	• **Name (E3 ligase):** NJH-04–087 (CRBN) • **Affinity:** IC$_{50}$ = 0.095 µM to Keap1 (TR-FRET) • **Cell:** degrade Keap1 @0.1–1 µM (MM.1S and NHBE cells)	113
48	• **Name (E3 ligase):** PROTAC 14 (CRBN) • **Affinity:** IC$_{50}$ = 0.046 µM to Keap1 (homogeneous time-resolved fluorescence, HTRF) • **Cell:** Keap1 degradation: DC$_{50}$ = 11 nM and D$_{max}$ = 94% @1 µM (HEK293T cells); DC$_{50}$ < 1 nM and D$_{max}$ = 90% @63 nM (BEAS-2B cells); upregulation of NQO1, HO-1 and/or GCLM @0.03–1 µM (HEK293T, HCA7, BEAS-2B, and A549 cells but less potent than racemic **34**/KI-696); up to fourfold induction @0.1–1 µM (ARE-luciferase reporter assay; HepG2; racemic **34**/KI-696 showed 3–6-fold induction); 2–5-fold upregulation of mRNA NQO1, TALDO1, and GCLM @0.13 µM (BEAS-2B); rescue from ROS-induced cell death: 50%–100% @4–500 nM (BEAS-2B cells; racemic **34**/KI-696: complete rescue at 1 nM)	114
49	• **Name (E3 ligase):** SD2267 (CRBN) • **Affinity:** K$_i$ = 57.7 nM to CRBN (FRET) • **Cell:** Keap1 degradation: DC$_{50}$ = 8.1 nM and D$_{max}$ = 82% @300 nM (HepG2); DC$_{50}$ = 17 nM and D$_{max}$ = 77% @300 nM (AML12); Keap1 half-lives (DT$_{50}$) = 2.6 and 2.2 h (HepG2 and AML12, respectively); 12–14-fold nuclear translocation of Nrf2 @300 µM (AML12); 1.5–2.5-fold nuclear translocation of Nrf2 @100 µM (HepG2); 2–30-fold upregulation of NQO1, HMOX1, GCLC and GCLM mRNA @100 nM (AML12 and HepG2 cells); reduction in ROS and increased viability (∼10%) @100–300 nM (AML12) •**DMPK/Tox:** *in vivo* PK (ICR mice): C$_{max}$ = 1.97 µg/mL; AUC = 468 µg*min/mL (IP, 3 mg/kg); C$_{max}$ = 0.172 µg/mL; AUC = 35.8 µg*min/mL (PO, 3 mg/kg) • ***In vivo* pharmacology:** APAP-induced liver injury mouse model (IP, 1/3 mg/kg; 2 h after APAP): ∼twofold reduction in serum AST and ALT; decrease of Keap1 and increase of Nrf2 and HO-1 in liver; GSH/GSSG ratio restored; reduction of phosphorylated JNK (sign of mitochondrial damage); decrease of DNA fragmentation and hepatic necrosis	115

(KI-696) and **3** in complex with Keap1 Kelch.[103,104] Compound **44** (S217879) showed an impressive affinity of 4.15 nM to the Keap1 Kelch domain in a direct SPR assay and exhibited strong capacity to induce Nrf2 translocation in U2OS cell lines with an EC_{50} of 23 nM. Various cell-based assays confirmed that **44** is a strong and selective bioactive Nrf2 activator, and a thorough profiling of *in vitro* and *in vivo* DMPK and toxicity properties showed it to be a sufficiently bioavailable and safe compound. Interestingly, while **44** had a relatively short half-life in mice blood (<30–45 min) following single oral administration, Nrf2-controlled genes were upregulated in the liver (and kidney) for 4–24 hours.[103] In the methionine and choline-deficient diet (MCDD) mouse model of NASH, administration of **44** (3 and 30 mg/kg/day, 2 weeks) reduced the NAFLD activity score (NAS) based on histology, showing both improved steatosis and lobular inflammation scores. Upregulation of the antioxidant response and downregulation of proinflammatory mediators in the liver were detected by genetic expression studies, and in a dose–response study, NAS scores were shown to be improved even at a low dose (≤1 mg/kg/day). Similar effects were obtained in the translationally superior diet-induced obesity (DIO) NASH model following an 8-week treatment period. **44** reduced biochemical NASH markers, liver inflammation, NAS, and liver fibrosis, without affecting food intake or body weight. RNA sequencing revealed clear upregulation of Nrf2-controlled antioxidant genes and suppression of NASH progression and fibrosis-related genes. Overall, this study provides strong preclinical evidence of Keap1 being a promising drug target for NASH. A follow-up study supports that conclusion, as **44** showed antisteatotic effects; less DNA damage, apoptosis, and inflammation; and inhibition of fibrogenesis in three-dimensional patient-derived precision-cut liver slices (PCLS) from patients of both sexes varying in the stages of metabolic fatty liver disease and diabetes status. Importantly, **44** showed much more pronounced effects and also exerted additional effects (e.g. antifibrogenesis) to those seen for the PPARα/δ agonist elafibranor, which has previously failed NASH clinical trials.[105]

Other Keap1-Nrf2 inhibitors

Following a thorough HTS and hit validation campaign by SPR and lead optimization, a novel tetrahydronaphthalene derivative bearing an α-fluoramide moiety was recently developed.[106] Compound **45** showed potent inhibitory activity and a favorable DMPK profile due to good solubility, high permeability, low clearance, and high plasma exposure after oral administration. Furthermore, **45** induced 4.6-fold increased expression of HO-1 in kidney tissue, making it a promising compound for studying the effects of Keap1 inhibition on CKD. X-ray crystallography revealed a unique binding mode to Keap1, where α-fluoramide facilitated interactions with two neighboring hydrogen bond donors (Gln530 and Ser555).

Keap1 PROTACs

Using PROTACs to hijack the cells' ubiquitin system has become a popular strategy to impair challenging drug targets. The concept is to make heterobifunctional molecules consisting of a ligand towards the protein of interest (POI) to be degraded and a ligand that binds to an E3 ligase attached via a linker. When the linker is optimized so that the PROTAC induces a favorable orientation between the POI and the E3 ligase, the E3 ligase, in complex with an E2 enzyme bearing ubiquitin, catalyzes the transfer of the degradation marker to the POI, which will then be detected and degraded by the proteasome.[107] Keap1's role as an E3 ligase substrate adaptor has been exploited in the design of PROTACs. The first was developed by Lu *et al.* in 2018, where they used a peptidic PROTAC hijacking Keap1 to degrade Tau in cells.[108] Additionally, a peptide-based homo-PROTAC was recently shown to degrade Keap1, activate Nrf2 gene expression, and inhibit the expression of fibrosis biomarker genes in hepatic stellate cells.[109] In support of that, a Keap1 degrading PROTAC based on CDDO was shown to inhibit hepatic steatosis, steatohepatitis, and fibrosis in both *in vitro* and *in vivo* models of non-alcoholic fatty liver disease (NAFLD).[110] Furthermore, several small-molecule PROTACs have been described where Keap1 is used to ubiquitinate and degrade BRD4, a protein involved in oncogenic gene expression. These PROTACs are composed of JQ1, a known BRD4 ligand, different Keap1 ligands (covalent CDDO, noncovalent **34**/KI-696, or THIQ derivatives), and various linkers.[58,111–113]

In addition to this, Keap1-targeting PROTACs made from noncovalent small-molecule Keap1-Nrf2 inhibitors have also been made, as detailed here and in Table 2. Du *et al.* designed several PROTACs by linking the potent Keap1 Kelch inhibitor **34** with cereblon (CRBN) or von Hippel-Lindau E3 ligase (VHL) ligands.[113] They also generated a homo-PROTAC based on **34**; however, this was inactive in the multiple myeloma cell line (MM.1S). One of the VHL-recruiting PROTACs was able to degrade Keap1 at 1–10 μM, but competition was observed between the two E3 ligases, VHL and Keap1, as VHL was also found to be degraded at the same concentrations. More promising were the CRBN-recruiting PROTACs, **46** (NJH-04–086) and **47** (NJH-04–087), which degraded Keap1 at low concentrations in MM.1S cells, a neuroblastoma cell line (IMR-32), and a lung epithelial cell line (NHBE) without affecting CRBN levels.[113]

Chen *et al.* designed several PROTACs that used CRBN to degrade Keap1.[114] Similar to Du *et al.*, they used **34** and thalidomide as the Keap1- and CRBN-binding ligands. However, they investigated a range of linkers varying in length and nature and used another attachment point on **34**. The best compound, **48** (PROTAC 14), potently degraded Keap1 at DC_{50} values around 11 nM and < 1 nM in HEK293T and BEAS-2B cells, respectively, with a hook effect starting > 1 μM and 63 nM. The BEAS-2B cells showed reduced basal levels of Keap1 expression, which may explain the lower DC_{50} value. Noticeably, **48** did not affect CRBN levels. **48** was able to upregulate the production of NQO1 and HO-1 in different cells, but at a lower level than the original Keap1 inhibitor **34**. The compound also showed the ability to rescue BEAS-2B cells from ROS-induced cell death, but again to a lesser extent than the original inhibitor.[114]

Finally, the first *in vivo* data of a Keap1-degrading PROTAC based on a noncovalent small-molecule Keap1 inhibitor were recently published.[115] Compound **49** (SD2267) is similar in structure to **48** (PROTAC 14) but has a linker one carbon longer. The authors explored the impact of **49** on hepatotoxicity and tested its activity within HepG2 and AML12 cells. Keap1 was

potently degraded, with DC_{50} values around 8.1 and 17 nM, respectively. Upregulation and nuclear translocation of Nrf2 were observed, together with increased expression of NQO1, HMOX1, GCLC, and GCLM at 100 nM, and increased viability and reduction of ROS in APAP-treated cells. PK studies showed exposure after IP administration and to some extent also after PO administration. Next, **49** was tested in an APAP-induced liver injury mouse model (IP, 1 and 3 mg/kg, 2 h after APAP). The activity seemed to be dose-dependent, but statistically significant effects were mostly observed at the highest dose. AST and ALT levels decreased in serum, Keap1 levels decreased, and HO-1 and Nrf2 expression was increased in liver. Moreover, recovery of GSH depletion was detected, as was an improvement of APAP-induced mitochondrial damage and a decrease of hepatic necrosis.[115]

Concluding remarks and outlook

Keap1 is a drug target for approved covalent Nrf2 activator and a promising target for noncovalent Keap1-Nrf2 inhibitors against diseases involving oxidative stress and inflammation. Due to markedly different off-target profiles, the pharmacodynamic effects and side effects of the two compound types will likely differ in the clinic. Noncovalent Keap1-Nrf2 inhibitors are considered by many as attractive alternatives to covalent compounds due to their higher specificity, which is expected to give a clearer mode of action and fewer side effects. Initially, medicinal chemistry has been challenged by the large and polar binding pocket of the Keap1 Kelch domain leading to less druglike compounds. These obstacles have been overcome in recent years by creative and persistent drug design efforts from both academia and industry. Different strategies such as screening, structure-based design, and FBDD have been implemented, and ROS-cleavable prodrugs, macrocycles, and PROTACs were recently successfully applied. Hence, today, several noncovalent Keap1-Nrf2 inhibitors exist showing high target-affinity, cell potency, selectivity, druglike DMPK properties, and activity in disease models (Tables 1 and 2). Noticeably, this has been achieved for molecules containing a carboxylic acid, demonstrating that, for example, high cell activity and oral availability can be combined despite this structural disadvantage present in most noncovalent Keap1-Nrf2 inhibitors. Alternatively, neutral bioisosteres and prodrugs have also shown promising results.

Many of the noncovalent Keap1-Nrf2 inhibitors described herein qualify as chemical probes useful for further studies of Keap1's role in pathophysiology. For example, compounds **12**, **34**, and **44** have been tested in off-target panels, suggesting a high degree of target specificity and selectivity as required for chemical probes. Some of the compounds, or derivatives thereof, could perhaps even serve as lead compounds for drug development. However, to our knowledge noncovalent Keap1-Nrf2 inhibitors have not yet entered clinical trials. Considering the sheer number and quality of the compounds described, many generated by companies, it may only be a matter of time. However,

some challenges remain (Figure 2); one is to find the right disease for clinical development, considering medical need, translational challenges, market potential, and the effect of Keap1 inhibition. Our detailed examination of the pharmacological effects in animal models elucidates some options. Several compounds (**10**, **16–18**, **30**) are effective in LPS-induced injury models in various tissues (colon, kidney, lung, heart) and APAP-induced hepatotoxicity (**13**, **21**, **49**) due to their antioxidative and antiinflammatory properties. Additionally, preclinical evidence from models of retinal I/R injury (**10**), COPD (**10**, **34**), and AD (**15**, **19**) makes these potential therapeutic areas. Finally, strong target validation data are available for NASH (**42**, **44**, PROTACs) and CKD, including Alport syndrome (**39**, **42**), where a robust link between Keap1-Nrf2 inhibition and amelioration of disease progression has been demonstrated.

To further advance noncovalent Keap1-Nrf2 inhibitors, it is crucial to investigate safety and toxicity more thoroughly considering both acute and long-term effects. Preferably, such studies will be conducted using standardized methods to facilitate comparison across laboratories. Additionally, structurally different compounds should be tested to allow discrimination between target-based and compound-specific toxicity. As part of assessing safety concerns, the functional outcome of potentially inhibiting the interaction between Keap1 and the noncanonical Keap1 Kelch-interacting proteins is a key question to study. Moreover, investigating the phase II metabolism of carboxylic acid-containing Keap1-Nrf2 inhibitors is relevant not only to understand the PK profile but also because carboxylic acids are prone to conjugation reactions, which can lead to reactive and toxic metabolites.

Overall, it seems that the field has reached a transition stage, where lead generation has proven possible and where more regulated drug development is the next logical step toward generating drug candidates for clinical trials. Only through this route can it be determined if noncovalent Keap1-Nrf2 inhibitors can provide safe and effective drugs in the future.

Declaration of interests

A.B. is coinventor on a patent application describing a new series of noncovalent Keap1-Nrf2 inhibitors. All other authors declare no interests.

Data availability

No data was used for the research described in the article.

Acknowledgements

References

1. Cuadrado A et al. Transcription factor NRF2 as a therapeutic target for chronic diseases: a systems medicine approach. *Pharmacol Rev*. 2018;70:348–383.

2. Casas AI et al. On the clinical pharmacology of reactive oxygen species. *Pharmacol Rev*. 2020;72:801–828.

3. Forman HJ, Zhang H. Targeting oxidative stress in disease: promise and limitations of antioxidant therapy. *Nat Rev Drug Discov*. 2021;20:689–709.

4. Pallesen JS, Tran KT, Bach A. Non-covalent small-molecule Kelch-like ECH-associated protein 1-nuclear factor erythroid 2-related factor 2 (Keap1-Nrf2) inhibitors and their potential for targeting central nervous system diseases. *J Med Chem*. 2018;61:8088–8103.

5. Baird L, Yamamoto M. The molecular mechanisms regulating the KEAP1-NRF2 pathway. *Mol Cell Biol*. 2020;40:e00099–e120.

6. Hayes JD, Dinkova-Kostova AT. The Nrf2 regulatory network provides an interface between redox and intermediary metabolism. *Trends Biochem Sci*. 2014;39:199–218.

7. Tonelli C, Chio IIC, Tuveson DA. Transcriptional regulation by Nrf2. *Antioxid Redox Signal*. 2018;29:1727–1745.

8. Cuadrado A et al. Therapeutic targeting of the NRF2 and KEAP1 partnership in chronic diseases. *Nat Rev Drug Discov*. 2019;18:295–317.

9. Dodson M, de la Vega MR, Cholanians AB, Schmidlin CJ, Chapman E, Zhang DD. Modulating NRF2 in disease: timing is everything. *Annu Rev Pharmacol Toxicol*. 2019;59:555–575.

10. Kobayashi EH et al. Nrf2 suppresses macrophage inflammatory response by blocking proinflammatory cytokine transcription. *Nat Commun*. 2016;7:11624.

11. Olagnier D et al. Nrf2 negatively regulates STING indicating a link between antiviral sensing and metabolic reprogramming. *Nat Commun*. 2018;9:3506.

12. Ma Q. Role of nrf2 in oxidative stress and toxicity. *Annu Rev Pharmacol Toxicol*. 2013;53:401–426.

13. Wardyn JD, Ponsford AH, Sanderson CM. Dissecting molecular cross-talk between Nrf2 and NF-kappa B response pathways. *Biochem Soc Trans*. 2015;43:621–626.

14. Thimmulappa RK et al. Nrf2 is a critical regulator of the innate immune response and survival during experimental sepsis. *J Clin Invest*. 2006;116:984–995.

15. Kim SW, Lee HK, Shin JH, Lee JK. Up-down regulation of HO-1 and iNOS gene expressions by ethyl pyruvate via recruiting p300 to Nrf2 and depriving It from p65. *Free Radic Biol Med*. 2013;65:468–476.

16. Soares MP et al. Heme oxygenase-1 modulates the expression of adhesion molecules associated with endothelial cell activation. *J Immunol*. 2004;172:3553–3563.

17. Kim JE, You DJ, Lee C, Ahn C, Seong JY, Hwang JI. Suppression of NF-kappa B signaling by KEAP1 regulation of IKK beta activity through autophagic degradation and inhibition of phosphorylation. *Cell Signal*. 2010;22:1645–1654.

18. Ogawa T, Ishitsuka Y. The role of KEAP1-NRF2 system in atopic dermatitis and psoriasis. *Antioxidants*. 2022;11:1397.

19. Naidu SD, Dinkova-Kostova AT. Omaveloxolone (SkyclarysTM) for patients with Friedreich's ataxia. *Trends Pharmacol Sci*. 2023;44:394–395.

20. Blewett MM et al. Chemical proteomic map of dimethyl fumarate-sensitive cysteines in primary human T cells. *Sci Signal*. 2016;9 rs10.

21. Piroli GG et al. Identification of novel protein targets of dimethyl fumarate modification in neurons and astrocytes reveals actions independent of Nrf2 stabilization. *Mol Cell Proteomics*. 2019;18:504–519.

22. Balak DM. Fumaric acid esters in the management of psoriasis. *Psoriasis (Auckl)*. 2015;5:9–23.

23. Brennan MS et al. Dimethyl fumarate and monoethyl fumarate exhibit differential effects on KEAP1, NRF2 activation, and glutathione depletion in vitro. *PLoS One*. 2015;10:e0120254.

24. Yadav SK, Soin D, Ito K, Dhib-Jalbut S. Insight into the mechanism of action of dimethyl fumarate in multiple sclerosis. *J Mol Med*. 2019;97:463–472.

25. Schulze-Topphoff U et al. Dimethyl fumarate treatment induces adaptive and innate immune modulation independent of Nrf2. *Proc Natl Acad Sci U S A*. 2016;113:4777–4782.

26. Prosperini L, Pontecorvo S. Dimethyl fumarate in the management of multiple sclerosis: appropriate patient selection and special considerations. *Ther Clin Risk Manag*. 2016;12:339–350.

27. Vollmer B et al. Discontinuation and comparative effectiveness of dimethyl fumarate and fingolimod in 2 centers. *Neurol Clin Pract*. 2018;8:292–301.

28. Cleasby A et al. Structure of the BTB domain of Keap1 and its interaction with the triterpenoid antagonist CDDO. *PLoS One*. 2014;9 e98896.

29. Yore MM, Kettenbach AN, Sporn MB, Gerber SA, Liby KT. Proteomic analysis shows synthetic oleanane triterpenoid binds to mTOR. *PLoS One*. 2011;6: e22862.

30. Liby KT, Sporn MB. Synthetic oleanane triterpenoids: multifunctional drugs with a broad range of applications for prevention and treatment of chronic disease. *Pharmacol Rev*. 2012;64:972–1003.

31. Wang YY, Yang YX, Zhe H, He ZX, Zhou SF. Bardoxolone methyl (CDDO-Me) as a therapeutic agent: an update on its pharmacokinetic and pharmacodynamic properties. *Drug Des Devel Ther*. 2014;8:2075–2088.

32. Chin MP et al. Mechanisms contributing to adverse cardiovascular events in patients with Type 2 diabetes mellitus and stage 4 chronic kidney disease treated with bardoxolone methyl. *Am J Nephrol*. 2014;39:499–508.

33. Horie Y et al. Molecular basis for the disruption of Keap1-Nrf2 interaction via Hinge & Latch mechanism. *Commun Biol*. 2021;4:576.

34. Davies TG et al. Monoacidic inhibitors of the Kelch-like ECH-associated protein 1:nuclear factor erythroid 2-related factor 2 (KEAP1:NRF2) protein-protein interaction with high cell potency identified by fragment-based discovery. *J Med Chem*. 2016;59:3991–4006.

35. Pallesen JS et al. Deconstructing noncovalent Kelch-like ECH-associated protein 1 (Keap1) inhibitors into fragments to reconstruct new potent compounds. *J Med Chem*. 2021;64:4623–4661.

36. Bradshaw PR, Athersuch TJ, Stachulski AV, Wilson ID. Acyl glucuronide reactivity in perspective. *Drug Discov Today*. 2020;25:1639–1650.

37. Weidolf L, Wilson I. Minimizing the DILI potential of carboxylic acid-containing drugs: a perspective. *Med Chem Res*. 2023;32:2034–2047.

38. Zhang Y, Shi Z, Zhou Y, Xiao Q, Wang H, Peng Y. Emerging substrate proteins of kelch-like ECH associated protein 1 (Keap1) and potential challenges for the development of small-molecule inhibitors of the Keap1-Nuclear factor erythroid 2-related factor 2 (Nrf2) protein-protein interaction. *J Med Chem*. 2020;63:7986–8002.

39. Hushpulian DM et al. Challenges and limitations of targeting the Keap1-Nrf2 pathway for neurotherapeutics: Bach1 de-repression to the rescue. *Front Aging Neurosci*. 2021;13 673205.

40. Dinkova-Kostova AT, Copple IM. Advances and challenges in therapeutic targeting of NRF2. *Trends Pharmacol Sci*. 2023;44:137–149.

41. Adamson R, et al. Human kelch-like ECH associated protein 1 (KEAP1); a target enabling package (TEP) (Version 1). 2019. https://doi.org/10.5281/zenodo.3246036

42. Crisman E et al. KEAP1-NRF2 protein-protein interaction inhibitors: Design, pharmacological properties and therapeutic potential. *Med Res Rev*. 2023;43:237–287.

43. MacLeod AK et al. Characterization of the cancer chemopreventive NRF2-dependent gene battery in human keratinocytes: demonstration that the KEAP1-NRF2 pathway, and not the BACH1-NRF2 pathway, controls cytoprotection against electrophiles as well as redox-cycling compounds. *Carcinogenesis*. 2009;30:1571–1580.

44. Casares L et al. The synthetic triterpenoids CDDO-TFEA and CDDO-Me, but not CDDO, promote nuclear exclusion of BACH1 impairing its activity. *Redox Biol*. 2022;51 102291.

45. Narayanan D et al. Development of noncovalent small-molecule Keap1-Nrf2 inhibitors by fragment-based drug discovery. *J Med Chem*. 2022;65:14481–14526.

46. Tran KT et al. A comparative assessment study of known small-molecule Keap1-Nrf2 protein-protein interaction inhibitors: chemical synthesis, binding properties, and cellular activity. *J Med Chem*. 2019;62:8028–8052.

47. Zhao Z, Dong R, Cui K, You Q, Jiang Z. An updated patent review of Nrf2 activators (2020-present). *Expert Opin Ther Pat*. 2023;33:29–49.

48. Zhao ZQ, Dong RT, You QD, Jiang ZY. Medicinal chemistry insights into the development of small-molecule kelch-like ECH-associated protein 1-nuclear factor erythroid 2-related factor 2 (Keap1-Nrf2) protein-protein interaction inhibitors. *J Med Chem*. 2023;66:9325–9344.

49. Hu L et al. Discovery of a small-molecule inhibitor and cellular probe of Keap1-Nrf2 protein-protein interaction. *Bioorg Med Chem Lett*. 2013;23:3039–3043.

50. Wen X, Thorne G, Hu L, Joy MS, Aleksunes LM. Activation of NRF2 signaling in HEK293 cells by a first-in-class direct KEAP1-NRF2 inhibitor. *J Biochem Mol Toxicol*. 2015;29:261–266.

51. Jnoff E et al. Binding mode and structure–activity relationships around direct inhibitors of the Nrf2–Keap1 complex. *ChemMedChem*. 2014;9:699–705.

52. Ontoria JM et al. Combined peptide and small-molecule approach toward nonacidic THIQ inhibitors of the KEAP1/NRF2 interaction. *ACS Med Chem Lett*. 2020;11:740–746.

53. Ma B et al. Design, synthesis and identification of novel, orally bioavailable non-covalent Nrf2 activators. *Bioorg Med Chem Lett*. 2020;30 126852.

54. Shi Z et al. Preparation of propionic acids containing 5-substituted tetrahydroisoquinoline and its application for treating or alleviating inflammatory disease. *CN114507181*. 2022.

55. Blaney EL et al. C4X Discovery Limited. Therapeutic compounds. WO2020084300A1.

56. Lucas CL, Ray NC, Seward EM, Hynd G. C4X Discovery Limited. Tetrahydroisoquinoline compounds as Nrf2 activators. WO2021214470A1.

57. Lucas CL et al. C4X Discovery Limited. Tetrahydroisoquinoline compounds as Nrf2 activators. WO2021214472A1.

58. Lucas CL, Ray NC, Esmieu WRK. C4X Discovery Limited. Preparation of tetrahydroisoquinoline compounds as KEAP1 binders. WO2023073364.

59. Marcotte D et al. Small molecules inhibit the interaction of Nrf2 and the Keap1 Kelch domain through a non-covalent mechanism. *Bioorg Med Chem*. 2013;21:4011–4019.

60. Jiang ZY et al. Discovery of potent Keap1-Nrf2 protein-protein interaction inhibitor based on molecular binding determinants analysis. *J Med Chem*. 2014;57:2736–2745.

61. Jain AD et al. Probing the structural requirements of non-electrophilic naphthalene-based Nrf2 activators. *Eur J Med Chem*. 2015;103:252–268.

62. Jiang ZY et al. Structure-activity and structure-property relationship and exploratory in vivo evaluation of the nanomolar Keap1-Nrf2 protein-protein interaction inhibitor. *J Med Chem*. 2015;58:6410–6421.

63. Lu MC et al. An inhibitor of the Keap1-Nrf2 protein-protein interaction protects NCM460 colonic cells and alleviates experimental colitis. *Sci Rep*. 2016;6:26585.

64. Lu MC et al. CPUY192018, a potent inhibitor of the Keap1-Nrf2 protein-protein interaction, alleviates renal inflammation in mice by restricting oxidative stress and NF-kappa B activation. *Redox Biol*. 2019;26 101266.

65. Hui QY et al. Inhibition of the Keap1-Nrf2 protein-protein interaction protects retinal cells and ameliorates retinal ischemia-reperfusion injury. *Free Radic Biol Med*. 2020;146:181–188.

66. Wang L et al. Developing a novel strategy for COPD therapy by targeting Nrf2 and metabolism reprogramming simultaneously. *Free Radic Biol Med*. 2021;169:436–445.

67. Lu MC et al. Polar recognition group study of Keap1-Nrf2 protein-protein interaction inhibitors. *ACS Med Chem Lett*. 2016;7:835–840.

68. Winkel AF et al. Characterization of RA839, a noncovalent small molecule binder to Keap1 and selective activator of Nrf2 signaling. *J Biol Chem*. 2015;290:28446–28455.

69. Lu MC et al. Discovery of a potent kelch-like ECH-associated protein 1-nuclear factor erythroid 2-related factor 2 (Keap1-Nrf2) protein-protein interaction inhibitor with natural proline structure as a cytoprotective agent against acetaminophen-induced hepatotoxicity. *J Med Chem*. 2019;62:6796–6813.

70. Lu MC, Shao HL, Liu T, You QD, Jiang ZY. Discovery of 2-oxy-2-phenylacetic acid substituted naphthalene sulfonamide derivatives as potent KEAP1-NRF2 protein-protein interaction inhibitors for inflammatory conditions. *Eur J Med Chem*. 2020;207 112734.

71. Sun Y et al. Direct inhibition of Keap1-Nrf2 protein-protein interaction as a potential therapeutic strategy for Alzheimer's disease. *Bioorg Chem*. 2020;103 104172.

72. Zhang L et al. Structure-based molecular hybridization design of Keap1-Nrf2 inhibitors as novel protective agents of acute lung injury. *Eur J Med Chem*. 2021;222 113599.

73. Liu G et al. Crystallography-guided optimizations of the Keap1-Nrf2 inhibitors on the solvent exposed region: from symmetric to asymmetric naphthalenesulfonamides. *J Med Chem*. 2022;65:8289–8302.

74. Yan J et al. Fragment-based discovery of azocyclic alkyl naphthalenesulfonamides as Keap1-Nrf2 inhibitors for acute lung injury treatment. *J Med Chem*. 2023;66:8267–8280.

75. Sun Y et al. A potent phosphodiester Keap1-Nrf2 protein-protein interaction inhibitor as the efficient treatment of Alzheimer's disease. *Redox Biol*. 2023;64 102793.

76. Buckpitt A et al. Naphthalene-induced respiratory tract toxicity: metabolic mechanisms of toxicity. *Drug Metab Rev*. 2002;34:791–820.

77. Richardson BG et al. Replacement of a naphthalene scaffold in kelch-like ECH-associated protein 1 (KEAP1)/nuclear factor (erythroid-derived 2)-like 2 (NRF2) inhibitors. *J Med Chem*. 2018;61:8029–8047.

78. Lazzara PR et al. Isoquinoline kelch-like ECH-associated protein 1-nuclear factor (erythroid-derived 2)-like 2 (KEAP1-NRF2) inhibitors with high metabolic stability. *J Med Chem*. 2020;63:6547–6560.

79. Naidu DS et al. The isoquinoline PRL-295 increases the thermostability of Keap1 and disrupts its interaction with Nrf2. *iScience*. 2022;25 103703.

80. Lazzara PR et al. Synthesis and evaluation of noncovalent naphthalene-based KEAP1-NRF2 inhibitors. *ACS Med Chem Lett*. 2020;11:521–527.

81. Abed DA et al. Optimization of 1,4-bis(arylsulfonamido)naphthalene-N, N'-diacetic acids as inhibitors of Keap1-Nrf2 protein-protein interaction to suppress neuroinflammation. *Bioorg Med Chem*. 2021;44 116300.

82. Abed DA, Lee S, Hu L. Discovery of disubstituted xylylene derivatives as small molecule direct inhibitors of Keap1-Nrf2 protein-protein interaction. *Bioorg Med Chem*. 2020;28 115343.

83. Georgakopoulos N et al. Phenyl bis-sulfonamide Keap1-Nrf2 protein-protein interaction inhibitors with an alternative binding mode. *J Med Chem*. 2022;65:7380–7398.

84. Lee S, Abed DA, Nguyen MU, Verzi MP, Hu L. Structure-activity relationships of 1,4-bis(arylsulfonamido)-benzene or naphthalene-N, N'-diacetic acids with varying C2-substituents as inhibitors of Keap1-Nrf2 protein-protein interaction. *Eur J Med Chem*. 2022;237 114380.

85. Abed DA, Ali AR, Lee S, Nguyen MU, Verzi MP, Hu L. Optimization of the C2 substituents on the 1,4-bis(arylsulfonamido)naphthalene-N, N'-diacetic acid scaffold for better inhibition of Keap1-Nrf2 protein-protein interaction. *Eur J Med Chem*. 2023;252 115302.

86. Sun YF et al. Design, synthesis and evaluation of novel small molecules acting as Keap1-Nrf2 protein-protein interaction inhibitors. *J Enz Inh Med Chem*. 2022;37:2575–2588.

87. Yasuda D et al. Discovery of benzo[g]indoles as a novel class of non-covalent Keap1-Nrf2 protein-protein interaction inhibitor. *Bioorg Med Chem Lett*. 2017;27:5006–5009.

88. Zhou HS et al. Design, synthesis, and structure-activity relationships of indoline-based kelch-like ECH-associated protein 1-nuclear factor (erythroid-derived 2)-like 2 (Keap1-Nrf2) protein-protein interaction inhibitors. *J Med Chem*. 2020;63:11149–11168.

89. Lu M, Zhang X, Zhao J, You Q, Jiang Z. A hydrogen peroxide responsive prodrug of Keap1-Nrf2 inhibitor for improving oral absorption and selective activation in inflammatory conditions. *Redox Biol*. 2020;34 101565.

90. Heightman TD et al. Structure-activity and structure-conformation relationships of aryl propionic acid inhibitors of the kelch-like ECH-associated protein 1/nuclear factor erythroid 2-related factor 2 (KEAP1/NRF2) protein-protein interaction. *J Med Chem*. 2019;62:4683–4702.

91. Norton D et al. Fragment-guided discovery of pyrazole carboxylic acid inhibitors of the kelch-like ECH-associated protein 1: nuclear factor erythroid 2 related factor 2 (KEAP1:NRF2) protein-protein interaction. *J Med Chem*. 2021;64:15949–15972.

92. Bewley MA et al. Opsonic phagocytosis in chronic obstructive pulmonary disease is enhanced by Nrf2 agonists. *Am J Respir Crit Care Med*. 2018;198:739–750.

93. Barbay JK et al. Janssen Pharmaceutica NV. Inhibitors of Keap1-Nrf2 protein-protein interaction. WO2020041169A2.

94. Miyabe T, Machida S, Oba Y. Senju Pharmaceutical Co., Ltd. Nrf2-activating compound. WO2021002473A1.

95. Komori K-I et al. UBE Industries, Ltd. Benzotriazole derivative. WO2020241853A1.

96. Kaseda S et al. Novel Keap1-Nrf2 protein-protein interaction inhibitor UBE-1099 ameliorates progressive phenotype in Alport syndrome mouse model. *Kidney360*. 2022;3:687–699.

97. Cummings MD, Sekharan S. Structure-based macrocycle design in small-molecule drug discovery and simple metrics to identify opportunities for macrocyclization of small-molecule ligands. *J Med Chem*. 2019;62:6843–6853.

98. Garcia Jimenez D, Poongavanam V, Kihlberg J. Macrocycles in drug discovery - learning from the past for the future. *J Med Chem*. 2023;66:5377–5396.

99. Begnini F et al. Mining natural products for macrocycles to drug difficult targets. *J Med Chem*. 2021;64:1054–1072.

100. Begnini F et al. Importance of binding site hydration and flexibility revealed when optimizing a macrocyclic inhibitor of the Keap1–Nrf2 protein–protein interaction. *J Med Chem*. 2022;65:3473–3517.

101. Matsumoto S et al. Scohia Pharma, Inc. Macrocyclic compound and use thereof. WO2020116660A1.

102. Barberis C, Karageorge G, Jurcak J, Terranova K. Sanofi. Tetrahydroisoquinoline derivatives for the treatment of red blood disorders and inflammatory diseases. WO2022056448A1.

103. Seedorf K et al. Selective disruption of NRF2-KEAP1 interaction leads to NASH resolution and reduction of liver fibrosis in mice. *JHEP Rep*. 2023;5 100651.

104. Wéber C et al. Les laboratoires Servier. New macrocyclic compounds, a process for their preparation and pharmaceutical compositions containing them. WO2021170774A1.

105. Hammoutene A et al. A new NRF2 activator for the treatment of human metabolic dysfunction associated fatty liver disease. *JHEP Rep*. 2023;5 100845.

106. Otake K et al. Methyl and fluorine effects in novel orally bioavailable Keap1-Nrf2 PPI inhibitor. *ACS Med Chem Lett*. 2023;14:658–665.

107. Hu Z, Crews CM. Recent developments in PROTAC-mediated protein degradation: from bench to clinic. *ChemBioChem*. 2022;23:e202100270.

108. Lu M et al. Discovery of a Keap1-dependent peptide PROTAC to knockdown Tau by ubiquitination-proteasome degradation pathway. *Eur J Med Chem*. 2018;146:251–259.

109. Wang F et al. Cell-Permeable PROTAC degraders against KEAP1 efficiently suppress hepatic stellate cell activation through the antioxidant and anti-Inflammatory pathway. *ACS Pharmacol Transl Sci*. 2023;6:76–87.

110. Qi M et al. Discovery of NAFLD-improving agents by promoting the degradation of Keap1. *J Med Chem*. 2023;66:9184–9200.

111. Tong B et al. Bardoxolone conjugation enables targeted protein degradation of BRD4. *Sci Rep*. 2020;10:15543.

112. Wei J et al. Harnessing the E3 ligase KEAP1 for targeted protein degradation. *J Am Chem Soc*. 2021;143:15073–15083.

113. Du G et al. Exploring the target scope of KEAP1 E3 ligase-based PROTACs. *Cell Chem Biol*. 2022;29:1470–1481.e31.

114. Chen H et al. Design and characterization of a heterobifunctional degrader of KEAP1. *Redox Biol*. 2023;59 102552.

115. Park SY et al. Development of KEAP1-targeting PROTAC and its antioxidant properties: In vitro and in vivo. *Redox Biol*. 2023;64 102783.

Reviews • KEYNOTE REVIEW